SPE-185025-MS

Quantitative Evaluation of Key Geological Controls on Regional Eagle Ford Shale Production Using Spatial Statistics

Yao Tian, Walter B. Ayers, Huiyan Sang, William D. McCain, Jr. Texas A&M University, and Christine Ehlig-Economides, University of Houston

This paper was prepared for presentation at the SPE Canada Unconventional Resources Conference held in Calgary, Alberta, Canada, 15—16 February 2017.

Abstract

Recent progress has increased our understanding of key controls on the productivity of shale reservoirs. The quantitative relations between regional Eagle Ford Shale production trends and geologic parameters were investigated to clarify which geologic parameters exercise dominant control on well production rates.

Previously, qualitative correlations for the Eagle Ford Shale were demonstrated among depth, thickness, total organic carbon (TOC), distribution of limestone beds, and average bed thickness with regional production. Eagle Ford production wells are horizontal, but it was necessary to use vertical wells that penetrated the Eagle Ford to map reservoir properties. No wells in the data base had both production and geological parameters, thus geological parameters could not be directly related to individual well production. Therefore, spatial interpolation methods based on kriging and Bayesian method with Markov Chain Monte Carlo (MCMC) sampling algorithms were utilized to integrate data sets and predict geological properties at production well locations. The spatial Gaussian Process regression modeling was conducted to investigate the primary controls on production.

Results suggest that the 6-month cumulative production from the Eagle Ford Shale, in barrels-of-oil equivalent (BOE), increases consistently with (a) depth, (b) Eagle Ford thickness (up to 180-ft thickness), and (c) with TOC (up to 7%). Also, when the number of limestone beds exceeds 12, production increases with the number of limestone beds. The corresponding significance code indicates that the parameters most significant to production are TOC and depth (which relates to pressure and thermal maturation).

Concepts and models developed in this study may assist operators in making critical Eagle Ford Shale development decisions and should be transferable to other shale plays.

[1] Yao Tian was with Texas A&M University, College Station, TX. She is now with University of Houston

Introduction

Shale gas and oil play significant roles in U.S. energy independence (EIA 2011; 2012; 2014; 2016). In 2014, crude oil proved reserves reached 39.9 billion barrels, and proved reserve of U.S. natural gas increased to 38.8 trillion cubic feet, setting the highest historical records for the second consecutive year (EIA 2015). After successful development of Barnett Shale in Fort Worth Basin, Haynesville Shale in Louisiana and Texas, and Marcellus Shale in Pennsylvania, the Eagle Ford Shale became among the most rapidly developing shale-gas plays in the U.S. (TRC 2014). In 2009, Eagle Ford Shale recoverable resources were estimated to be 21 trillion cubic feet natural gas and 3 billion barrels of shale oil (EIA 2011).

The Eagle Ford Shale dips southeastward from outcrop; depth exceeds 13,000 ft at the Sligo Shelf Margin (**Fig. 1**) (Hentz and Ruppel 2010; Tian, et al. 2012). The Eagle Ford Shale is divided into 3 units. The Lower Eagle Ford is present throughout the study area; it is more than 275 ft thick in the Maverick Basin depocenter and thins to less than 50 ft on the northeast (**Fig. 2**) (Tian et al. 2012). The TOC of the lower Upper Eagle Ford Shale is greatest (7%) in Zavala and Frio Counties (Tian et al. 2012). A strike-elongate trend of high TOC, high average gamma ray responses, and low bulk density extends from Maverick County northeast through Guadalupe County, parallel to and updip of the Sligo and Stuart City Shelf Margins (**Fig. 3**) (Tian et al. 2013). The numbers of both limestone and organic-rich marl (ORM) beds, which together comprise the Eagle Ford Shale, increase from fewer than 2 near outcrop in the northwest to more than 20 on the southeast at the Sligo Shelf Margin (**Fig. 4**). Average thickness of limestone and ORM beds in the Lower Eagle Ford Shale is low (< 5 ft.) in the La Salle – DeWitt trend, coincident with the most productive gas and oil regions, respectively (**Fig. 5**) (Tian et al. 2014).

Having characterized the key geological parameters that may affect Eagle Ford production, the questions remained: “Is there a quantitative relationship between production and the above parameters?” And, if so, “Which geological parameter has the dominant control on production?”

The difficulty of relating geological parameters to production occurs because no wells in the data base have both production and geological data. The wells used to calculate geological parameters are vertical wells that were drilled for reservoirs below the Eagle Ford Shale. However, the production wells are horizontal wells. Therefore, production data cannot be directly related to geological data at individual well locations.

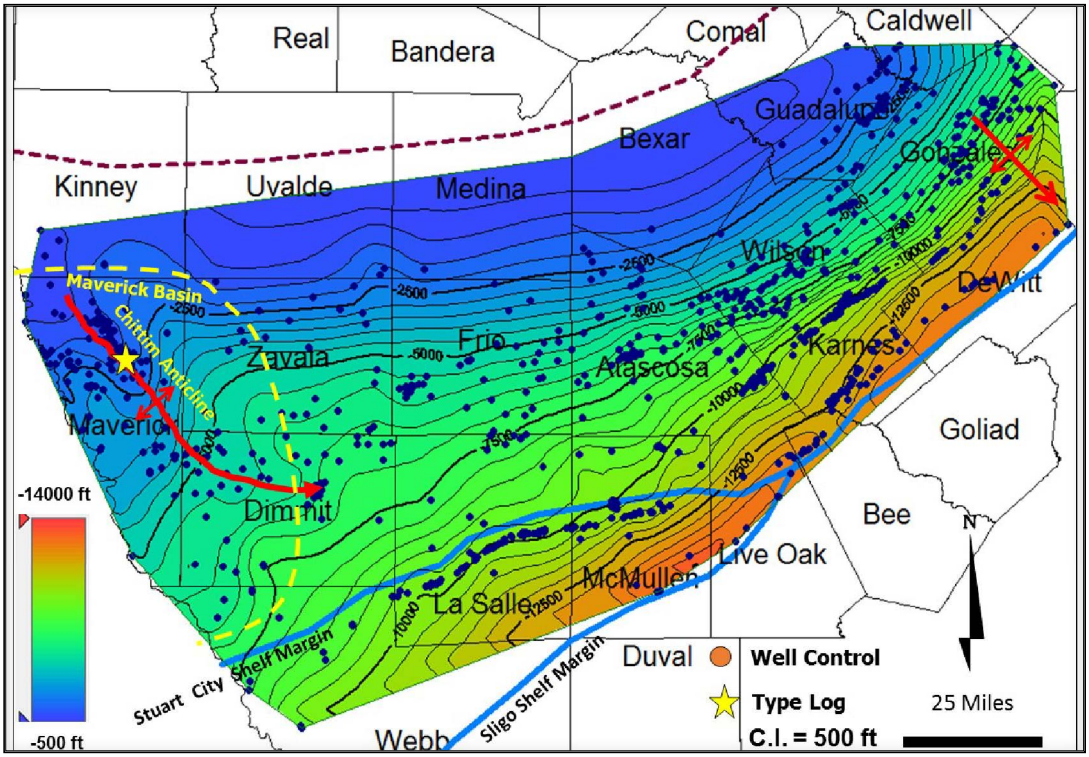

Fig. 1 Structural Base of Lower Eagle Ford Shale (Tian et al. 2012). Republished by permission of the Gulf Coast Association of Geological Societies, whose permission is required for further publication use.

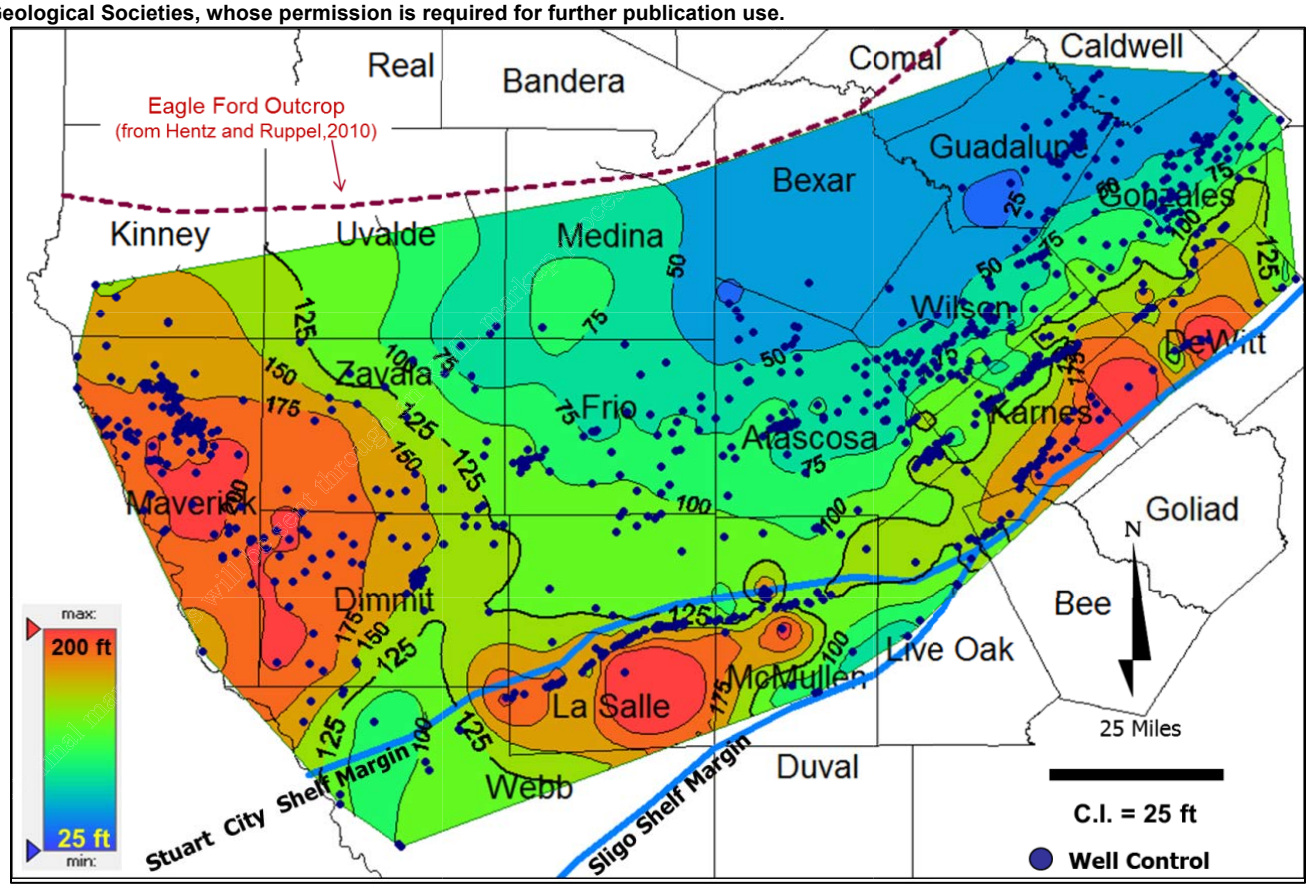

Fig. 2 Thickness of Lower Eagle Ford Shale (Tian et al. 2012). Republished by permission of the Gulf Coast Association of Geological Societies, whose permission is required for further publication use.

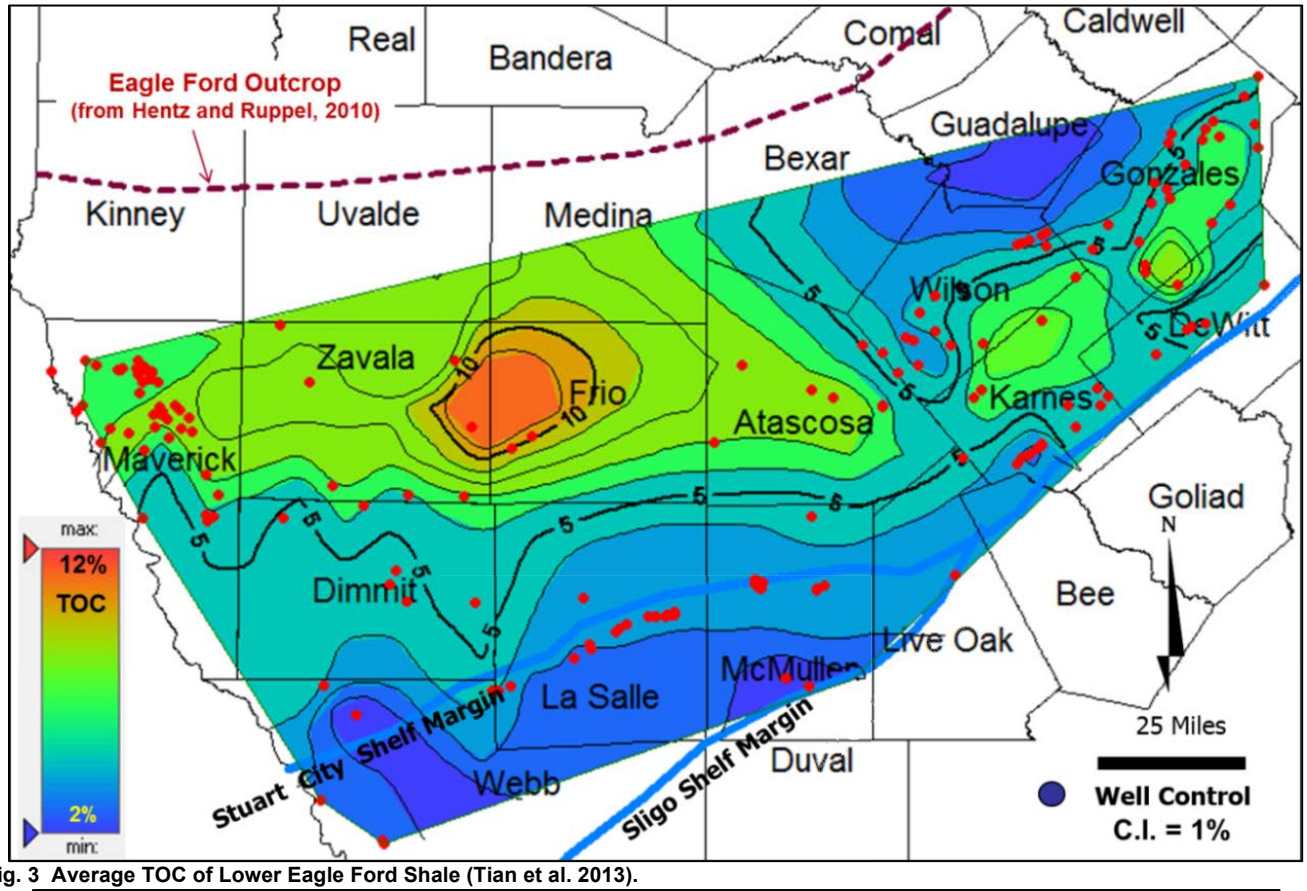

Fig. 3 Average TOC of Lower Eagle Ford Shale (Tian et al. 2013).

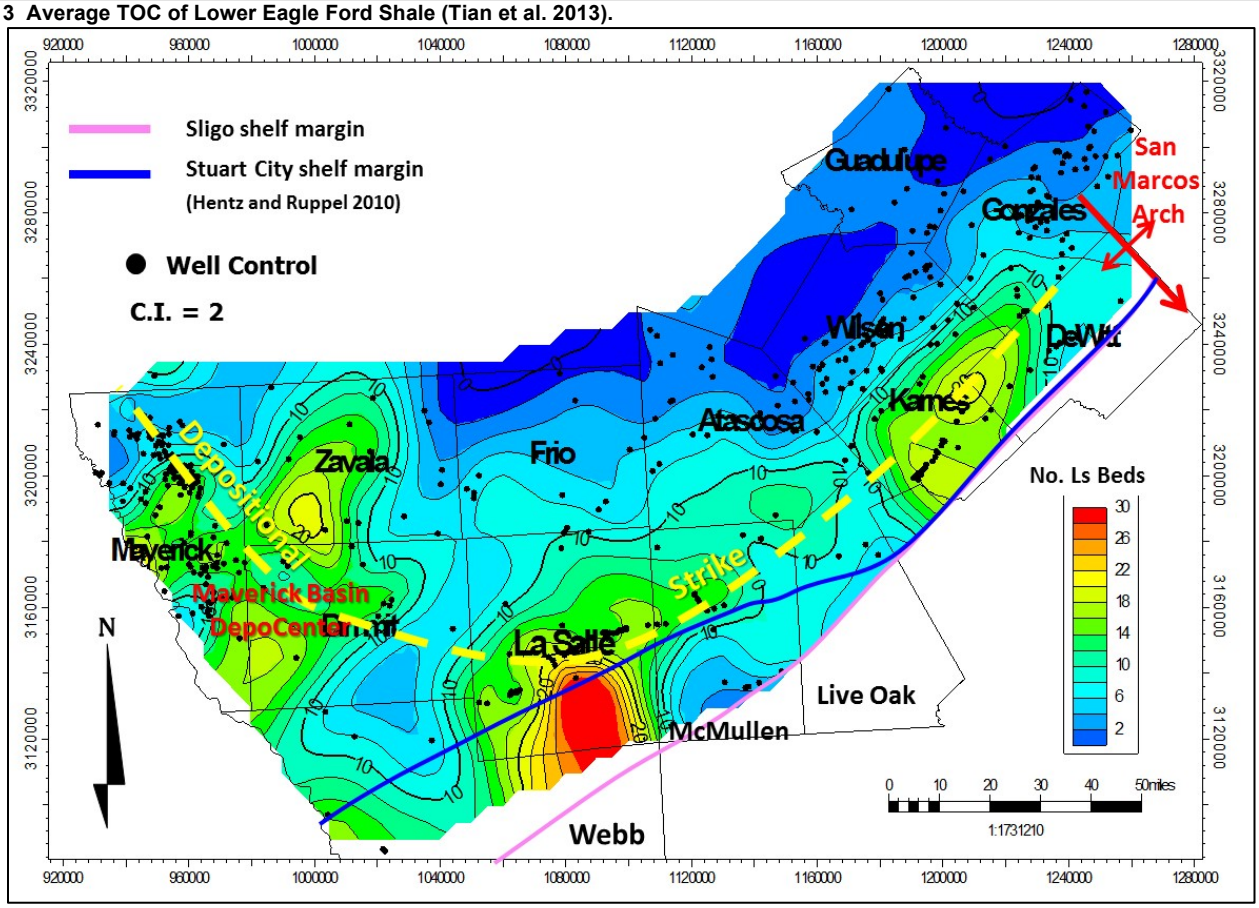

Fig. 4 Number of limestone beds of Lower Eagle Ford Shale (Tian et al. 2014).

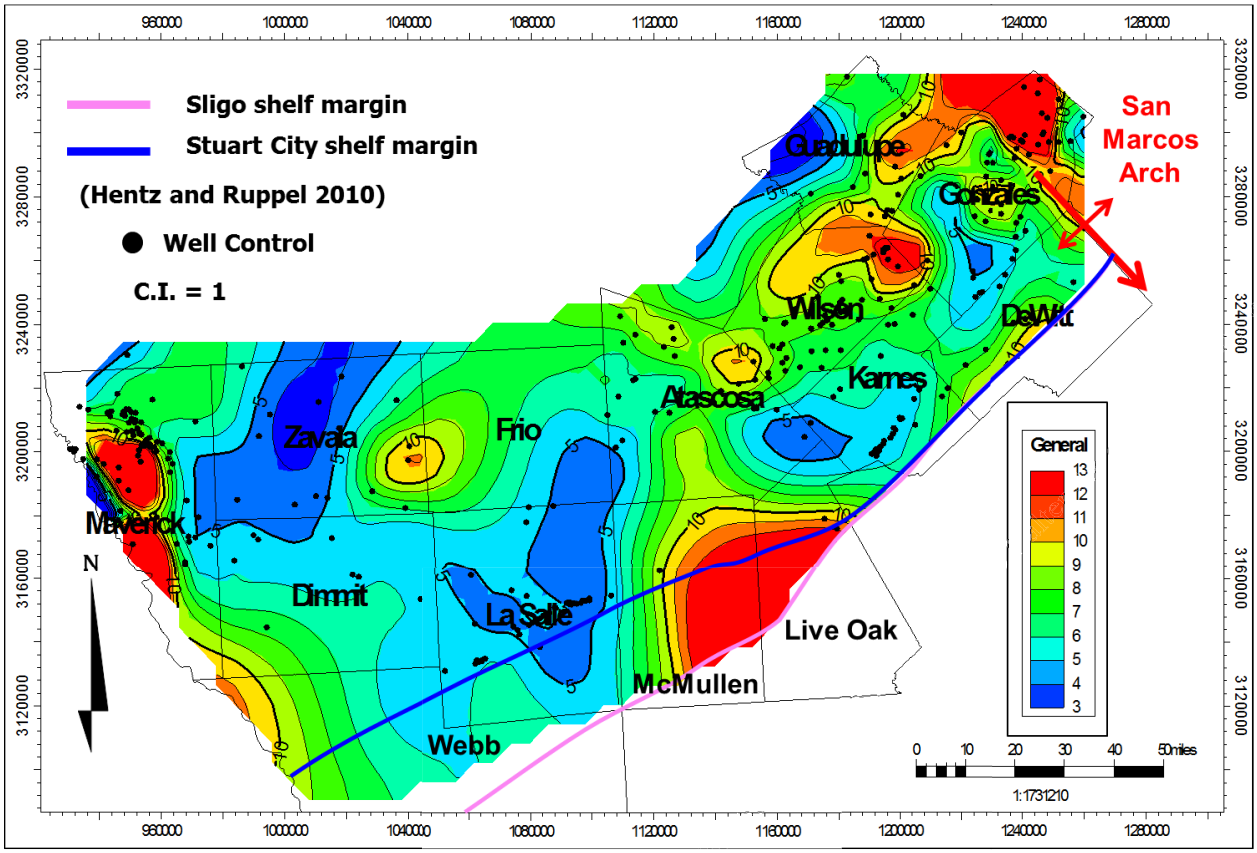

Fig. 5 Average bed thickness of Lower Eagle Ford Shale (Tian et al. 2014).

Methods

As mentioned, one of the challenges of correlating the impact of geological parameters with production relates to the misalignment between horizontal producers and geological data from nearby vertical wells. Wells with complete measurements in our data base are quite limited. The data base has both vertical deeper well logs that penetrate Eagle Ford Shale but do not have Eagle Ford production, and Eagle Ford horizontal wells that do not penetrate the full formation but have production data. Therefore, interpolation of reservoir properties from vertical well locations to horizontal wells is required. An estimated spatial covariance function is crucial to achieving an accurate interpolation. Identifying the distribution pattern for each variable is the key to selecting the correct method to fit the covariance function. The following workflow was designed to characterize the distributional differences among various data sets. Coefficients and p-values obtained from a spatial Gaussian process model were analyzed to determine the relative significance of the geologic parameters to production.

Input Parameter Selection

Previous publications have listed the screening criteria for shale oil and gas plays (Hill and Nelson 2000; Wang and Gale 2009). Shale gas characterization plays a significant role in gas-in-place calculation and completion design, both of which have strong impacts on well overall productivity. Among the geologic factors that directly affect shale oil and gas production are thermal maturity, formation pressure, thickness, TOC, gas content, porosity, and brittleness (Hill and Nelson 2000; Curtis, 2002; Bowker 2003, 2007; Montgomery et al. 2005; Jarvie et al. 2007; Pollastro et al. 2007; Rickman et al. 2008; Wang and Gale 2009; Spears and Jackson 2009; Passey et al. 2010; Cipolla et al. 2011).

Researchers have divided those key parameters in two categories, including depth-depend and non-depth dependent (Wang and Gale 2009). Temperature, pressure and thermal maturity increase with depth; therefore, the free gas and absorbed gas volume are strongly related to depth. Rock brittleness depends on a variety of parameters including effective stress, mineralogy, TOC, reservoir temperature, and diagenesis, many of which are functions of depth (Handin and Hagar 1957; Handin et al. 1963;

Davis and Reynolds 1996; Wang and Gale 2009). Thermal maturity increases with depth in the Eagle Ford Shale (Wang and Gale 2009; Tian and Ayers 2012). Organic richness (TOC) is a critical source rock quality parameter (Passey et al. 1990; Passey et al. 2011). TOC serves as an indicator of hydrocarbon generation potential, which is regarded as excellent if TOC exceeds 4% (Peters and Cassa 1994; Baskin 1997). In addition to controlling the hydrocarbon generation potential, TOC is important to reservoir quality by affecting absorption capacity, water saturation, and porosity (Passey et al. 2010; Dicman and Vernik 2013; Loucks and Reed 2014).

The unique characteristics presented by the shale gas reservoirs leads to the major shift from the traditional petrophysical workflow. The challenges are mainly attributed to the presence of organic material, complex mineral composition, and the multiple pore types and complex distributions in both organic and inorganic constituents (Passey et al. 2010). Because core analyses provide the ground truth for validation of reservoir properties, XRD, crushed-core GRI, and TOC analysis are particularly indispensable in shale assessment (Quirein et al 2010; Passey et al. 2010; Sondergeld et al. 2010; Ramirez et al 2011; Sun et al. 2015). Full characterization of shale reservoirs requires a comprehensive set of logging suite and core data to fully capture the heterogeneity and complexity of the formation (Quirein et al 2010; Passey et al. 2010; Sondergeld et al. 2010; Ramirez et al 2011; Quirein et al 2013; Sun et al. 2015).

However, neither laboratory measurements nor dipole sonic were available for this study, which made it impossible to achieve porosity or water saturation to determine the fluid volumetrics. Furthermore, rock mechanical properties such as Young's modulus, Poisson's ratio, and Brittleness index were unavailable (Rickman et al. 2008; Mullen et al. 2010; Quirein et al 2010; Passey et al. 2010; Sondergeld et al. 2010; Ramirez et al 2011; Cipolla et al. 2011; Wan et al. 2013; Huang et al. 2013; Yu et al. 2014; Huang and Torres-Verdin 2015; Sun et al. 2015). Therefore, we used alternative methods to represent such properties. In our study, TOC was employed to represent the reservoir quality, assuming its correlation with water saturation and porosity will hold true for the entire Eagle Ford play (Passey et al. 2010). Lithologic variability was used to indirectly characterize completion quality and potential for successful hydraulic stimulation. The Lower Eagle Ford consists of cyclic, interbedded organic-rich marl and limestone. The high gamma ray interval is regarded as good source rock and, potentially, good reservoir rock (Rickman et al. 2008; Mullen et al. 2010; Cipolla et al. 2011; Wan et al. 2013). Low gamma ray (brittle carbonate) intervals are better completion targets, which is key to successful development (Richman et al. 2008; Mullen et al. 2010; Cipolla et al. 2011). The number of limestone beds and average bed thickness were chosen to define the potential of for quality completions.

The reservoir parameters of depth, thickness, TOC, number of limestone beds, and average bed thickness of Lower Eagle Ford were selected for analysis. Mapping these properties and integrating them with the first 6 months production showed qualitative correlations among geologic parameters and production volumes in the highly production regions.

Data Preparation

Figure 6 summarizes the data preparation steps. The first step is to identify the distribution pattern. A histogram and a Q-Q plot (Q = quartile) plot were used to determine the type of distribution of each observed variable. The skewness was checked and the Box-Cox transformation was applied to transform the continuously distributed data into perfect Gaussian distributions (Box and Cox 1964). Spatial covariance models were then applied to fit these data and conduct spatial interpolation using kriging. Otherwise, the discretely distributed number of limestone beds were assumed to follow a Poisson distribution. Bayesian method with Markov Chain Monte Carlo (MCMC) sampling algorithms were utilized to integrate Poisson distribution data sets and predict geological properties at production well locations.

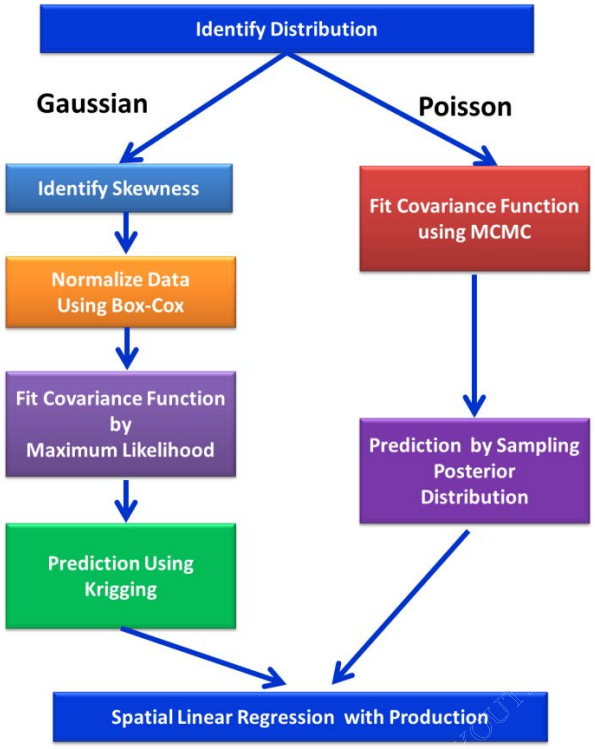

Fig. 6 Schematic workflow for quantifying influences on production from various geological parameters.

Skewness Identification

Distributions identified as Gaussian may need additional processing. A Q-Q plot is a graphical diagnostic tool used to analyze the shape of the distribution and skewness of the data by comparing the quantiles of two different distributions (Wilk and Gnanadesikan 1968). The geological parameters were plotted against randomly generated normal distribution data. If the distributions are similar, then a unit slope results (**Fig. 7**). Curvature on the Q-Q plot suggests that the distribution is skewed and requires normalization (Fig. 7) (Wilk and Gnanadesikan 1968).

Data Normalization

After skewness was identified with the Q-Q plot, a Box-Cox conversion was used to transform the data into a perfect Gaussian distribution. A Box-Cox transformation is defined as a continuous function with the power parameter, λ, which can transform the original data into Gaussian distribution (**Eq.1**) (Box and Cox 1964). A list of power parameters, λ, is generated and a profiled log-likelihood vector is computed, then the most likely λ can be determined by the maximum correlation coefficient (Box and Cox 1964; Scott 2008). A power parameter, λ, close to 1 suggests a Gaussian distribution, thus does not require the data to be transformed. If the value of λ from the Box-Cox analysis is close to zero, a log transformation will modify the data into a Gaussian distribution (Gelfand et al. 2010):

$$y_i^{(\lambda)} = \begin{cases} \dfrac{y_i^{\lambda} - 1}{\lambda}, if\ \lambda \neq 0 \\ \log(y_i), if \lambda = 0 \end{cases}. \quad (1)$$

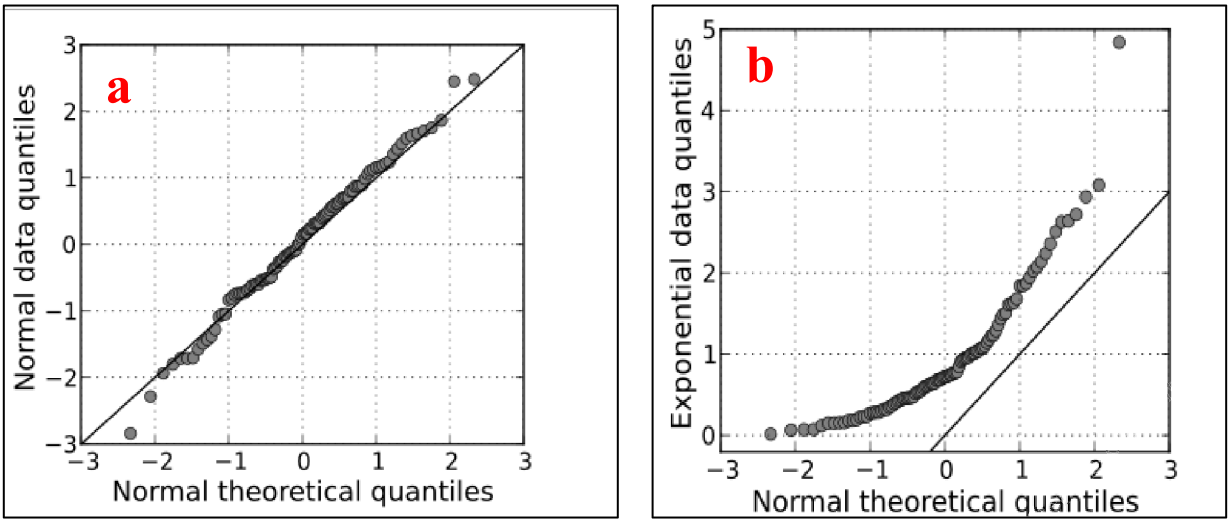

Fig. 7 (a) Unit slope on Q-Q plot for Gaussian distribution; (b) Curved pattern on Q-Q plot, suggesting skewness (Skbkekas 2009).

Covariance Function Fitting and Spatial Prediction for Gaussian Data

After transforming the Eagle Ford datasets into normally distributed variables, the spatial Gaussian process covariance models for spatial interpolation were adopted. The Maximum likelihood estimation method was used to fit the covariance models to obtain estimates of key covariance parameters. Specifically, a Gaussian data set can be modeled as below (Eq.2) (Gelfand et al. 2010):

$$Y(x) = \mu(x) + S(x) + e, \tag{2}$$

where x denotes a spatial location, μ(x) is the mean value of the data set, Y(x) is the observed geological data, S(x) is a spatial random effect modeled by a Gaussian process with a covariance function to capture spatial dependence, and e is the error term. A commonly used covariance function takes the following form (Eq.3) (Gelfand et al. 2010):

$$\mathrm{K(x)} = \alpha \left(\frac{x}{\beta}\right)^{\nu} \kappa_{\nu} \left(\frac{x}{\beta}\right), \tag{3}$$

where K(x) is the covariance function, α is the sill, β is the spatial range, ν is the smoothness parameter, and κ_{ν} is the Bessel function of second kind (Gelfand et al. 2010). Maximum likelihood estimations were used to estimate sill, range, and the smoothness parameters. By plugging in the estimated covariance parameters, an estimated covariance function for specific data set was obtained.

Kriging, the best linear unbiased prediction for spatial statistics (Krige and Kleingeld 2005; Rivoirard 2005; Gelfand et al. 2010), is widely applied in the oil and gas industry in building approximations of certain attributes from known points to wider areas. For the Gaussian distribution data set, conventional kriging was used to predict the geological data for production (horizontal) well locations, on the basis of nearby vertical wells. After fitting the data with the covariance model described, we can use conventional kriging to make spatial predictions of thickness at the production locations (horizontal wells), on the basis of the thickness controls of nearby vertical wells.

Poisson Distribution Data Prediction

Previous studies used covariance models for fitting and spatially predicting Gaussian data. However, many non-Gaussian spatial variables such as the number of limestone beds have been represented as discrete counts (Boham and Zech 2010; Gelfand et al. 2010). For non-Gaussian spatial variables,

covariance functions will not directly apply (Finley and Banerjee 2010). Instead, a hierarchical model serves as an alternative.

For example, a hierarchical model can be used to predict the number of limestone beds for horizontal well locations. The hierarchical model consists of two stages given by the following Eqs. 4 and 5 (Gelfand et al. 2010). In the first stage, the number of limestone beds at location S is modeled as a Poisson distribution with intensity $\lambda(s)$. In the second stage of the model, the non-Gaussian data $\lambda(s_i)$ at specific site, S_i, is transformed to a Gaussian latent process $\eta(s_i)$ plus a variable (β). In the Gaussian process $\eta(s_i)$ has a mean of zero, a variance of σ^2, and a latent spatial range of ϕ:

$$\eta(s_i) \sim N[0;\ \sigma^2 R(\phi)], \tag{4}$$

$$\log[\lambda(s_i)] = \beta + \eta(s_i). \tag{5}$$

The hierarchical model uses a Bayesian method to estimate the parameters and make predictions. The Bayesian method draws samples from the posterior of the distributions for parameters β, σ^2, and ϕ. Then values at new locations are inferred from the posterior model parameter samples. We proceeded with the Bayesian inference for the hierarchical model using the rigorous Markov Chain Monte Carlo (MCMC) method for the essential sampling process. The MCMC method is a computationally intensive yet robust sampling algorithm to generate samples based on a certain posterior distribution. Three chains of data with different starting values were generated for each set of values for β, variance of σ^2, and the latent spatial range of ϕ. The goal is to construct sample chains that converge to the desired distribution (Robert and Casella 2004; Zhang and Srinivasan 2005; Gelfand et al. 2010).

The computation above was carried out by the R statistical software platform. Available functions and tool packages in R enable specifying input data and prior models for model parameters without lengthy codes and subsequent fitting and prediction using a non-Gaussian regression model. Finley and Banerjee (2013) introduced the spatial generalized linear model (SPGLM) function specifically designed for hierarchical modeling for non-Gaussian spatial data in R. Their function fits the univariate Bayesian generalized linear spatial regression model and obtains β, σ^2, and ϕ by generating model parameters with MCMC methods (Banerjee, et al. 2004; Banerjee et al. 2008; Finley et al. 2015). With the posterior samples of β, σ^2, and ϕ obtained from SPGLM, we predict the number of limestone beds for new location with SPpredict, the function designed by Finley and Banerjee to collect the posterior and generate predictive samples at new locations (Banerjee et al. 2004; Finley et al. 2015). Banerjee et al. 2004; Roberts and Rosethal 2006; Banerjee et al. 2008; Finley et al. 2008; Finley et al. 2015 provided comprehensive descriptions of these algorithms.

Application

The primary production data set is the barrel of oil equivalent (BOE) of Eagle Ford first six months of production. It includes data from approximately 3,000 wells in 13 counties (**Fig. 8**). There is a northeast to southwest trend of production. Maximum production is in the central area of the production belt (Fig. 8).

We evaluated five geological parameters: structural elevation (Fig. 1), thickness (Fig. 2), TOC (Fig. 3), number of limestone beds (Fig. 4), and average bed thickness (Fig. 5). We divided the geological parameters into two types of distributions: Gaussian distributions and Poisson distributions. Depth, thickness, average layer thickness, and TOC follow a Gaussian distribution, whereas the number of limestone beds follow a Poisson distribution. The criterion for selecting these five parameters was their qualitative correlation with the first 6 months cumulative production.

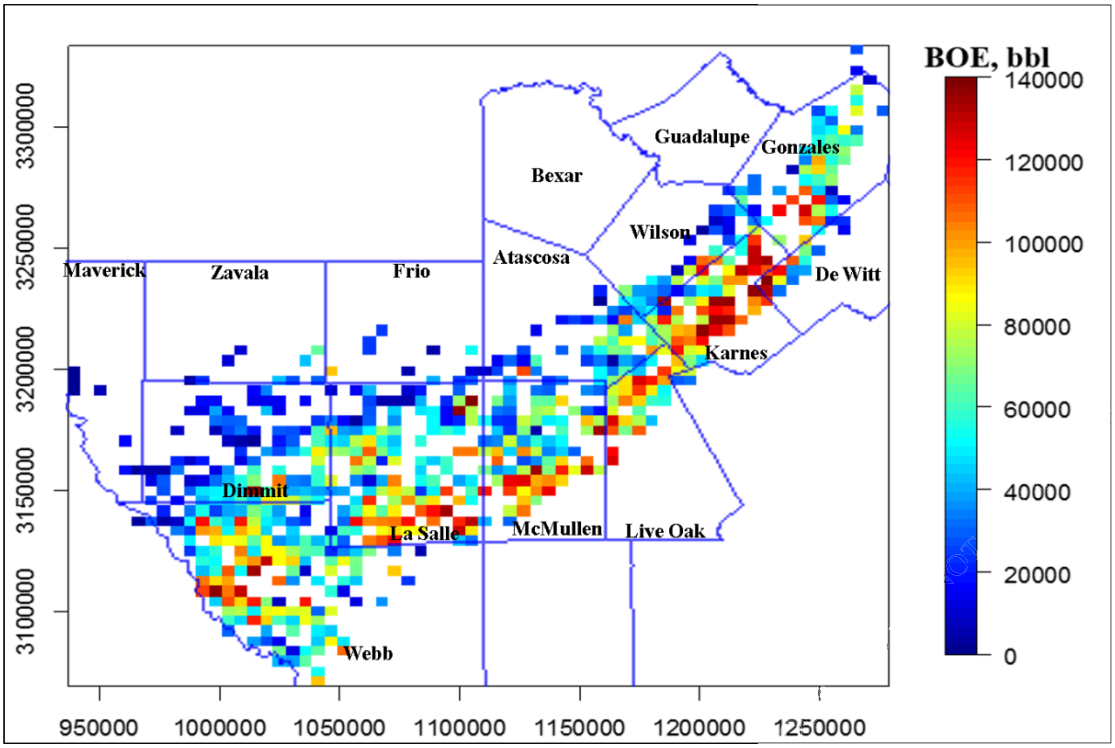

Fig. 8 Spatial map of first 6 months of production (BOE) of Eagle Ford Shale in South Texas. Coordinates uses North American Datum 1927 (NAD27) in meters.

Gaussian Data Group Prediction

The histogram and Q-Q plot show that depth data generally follow a Gaussian distribution (**Fig. 9**), and Box-Cox analyses indicate that λ is approximately 0.93. The histogram and Q-Q plot show that thicknesses, TOC, and average bed thickness in the Lower Eagle Ford generally follow power normal distribution (**Fig. 10**). The approximate Box-Cox analysis λ value of 0.2 for thickness suggests that log transformation of the original thickness can effectively eliminate the skewness, thereby following a Gaussian distribution (Fig. 10) confirmed by the unit slope of the Q-Q plot after the transformation (**Fig. 11**). Both TOC and average bed thickness show skewness on the Q-Q plots (Fig. 11). The skewness shown by average bed thickness was eliminated by power transformation using 0.75, whereas TOC was transformed by log transformation (Fig. 11). After transforming the data to Gaussian distribution without skewness, we used the Likfit function in the R software to estimate the spatial covariance model including sill, range, and smoothness parameters by achieving the maximum likelihood value. Ribeiro and Diggle (2016) introduced full details of the algorism employed in the Likfit function in their R software package geoR. After specifying sill, spatial range, and smoothness parameters from the vertical well locations for each Gaussian dataset, we predicted depth, thickness, average bed thickness, and TOC for Eagle Ford horizontal wells (**Figs. 12 through 19**).

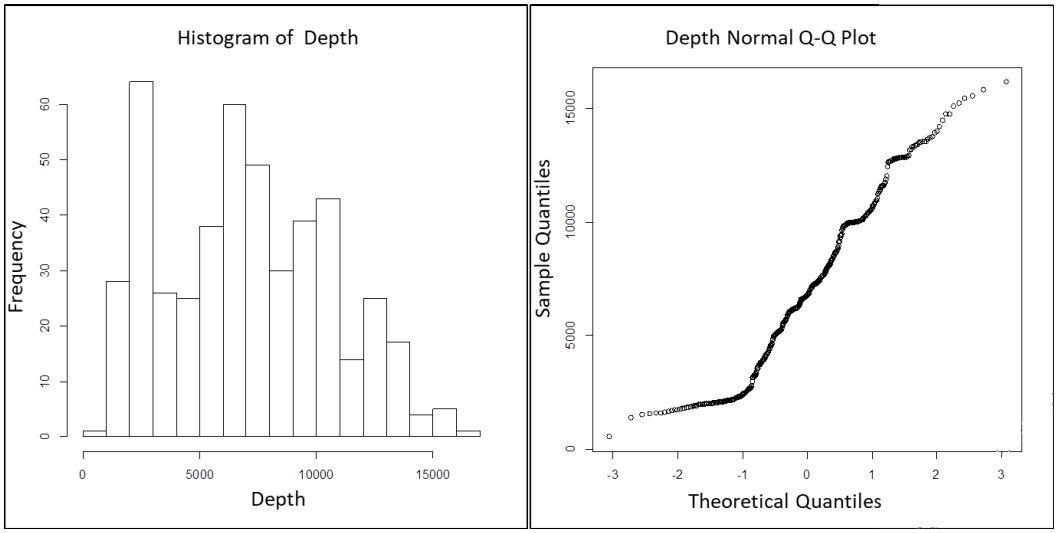

Fig. 9 Histogram and Q-Q plot of Eagle Ford Shale depth data.

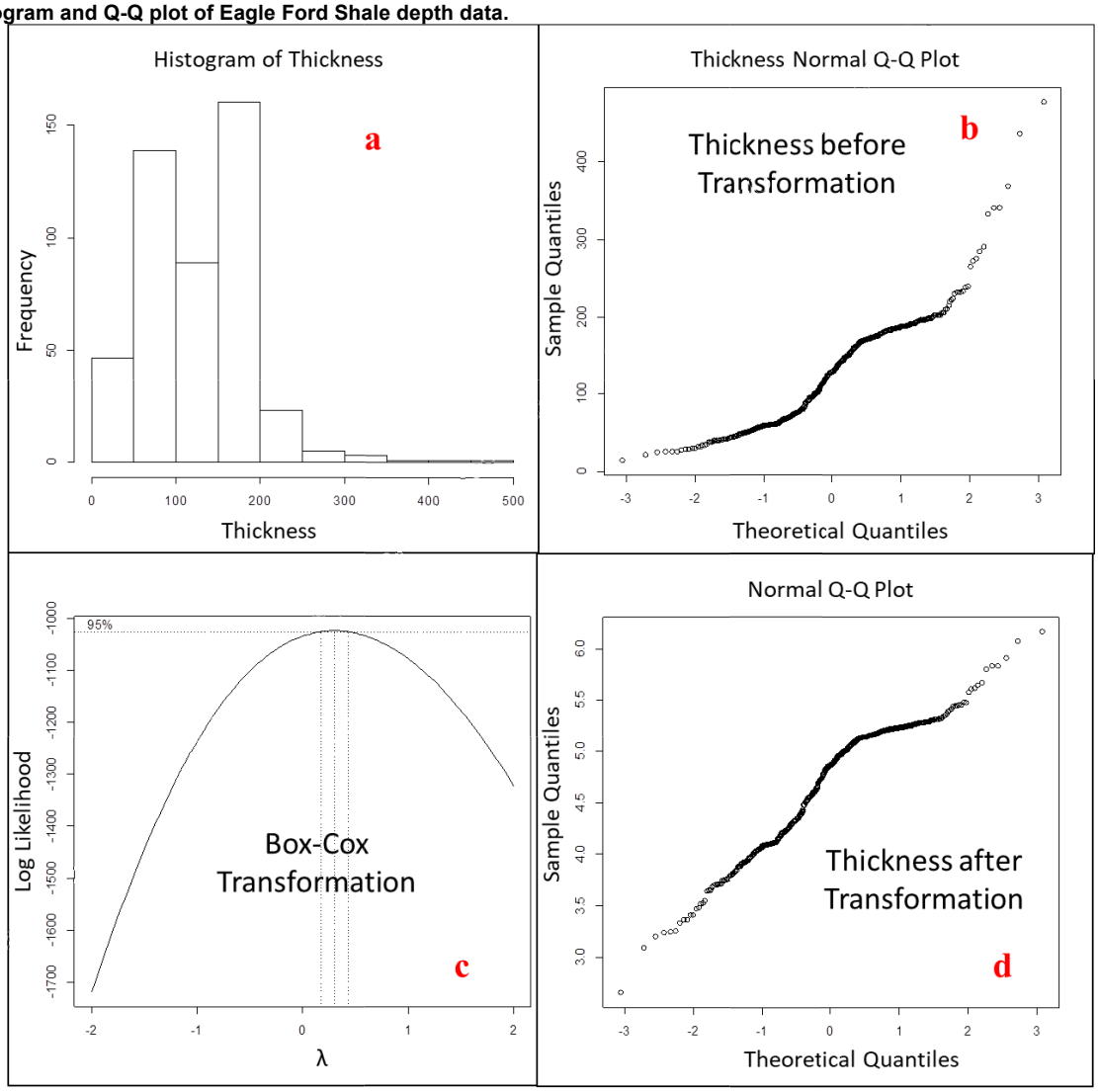

Fig. 10 (a) Histogram of thickness of Lower Eagle Ford Shale, (b) Q-Q plot of thickness, (c) Box-Cox transformation result, and (d) Q-Q plot of thickness data after Box-Cox transformation.

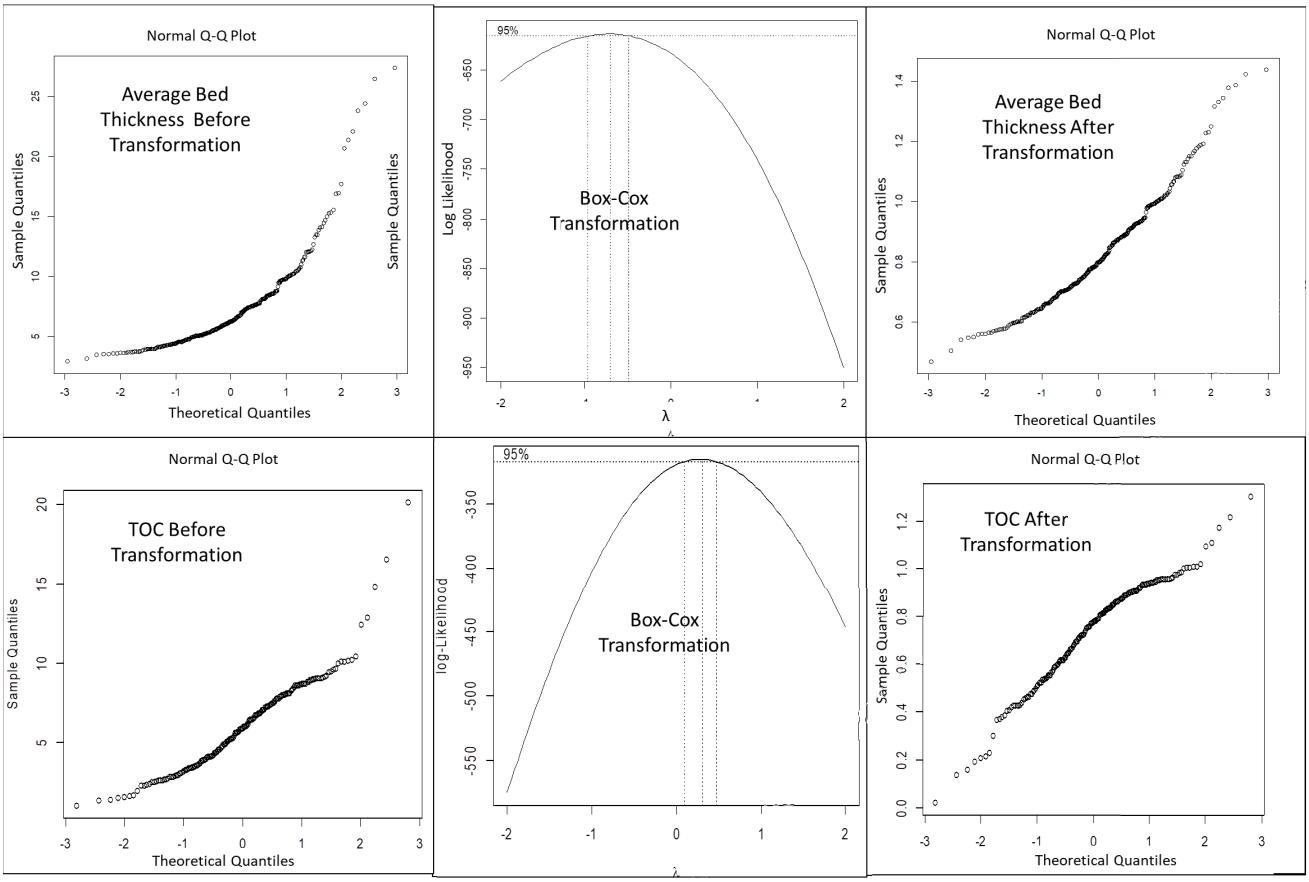

Fig. 11 Skewness elimination workflow by Q-Q plots and Box-Cox transformation.

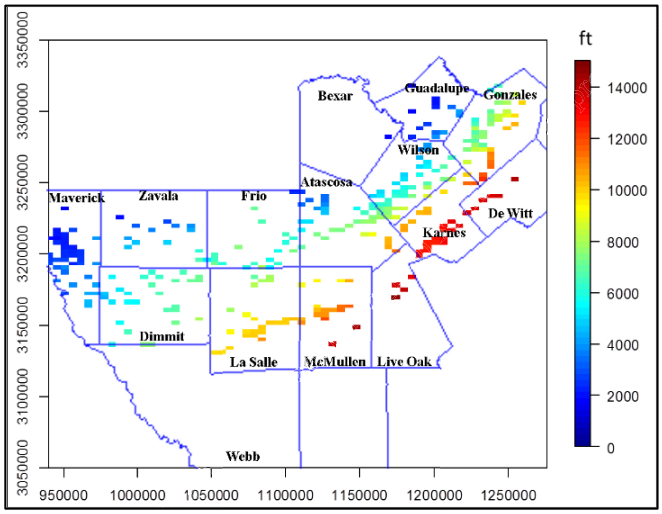

Fig. 12 Depth of Lower Eagle Ford Shale base by stratigraphic analyses on vertical wells.

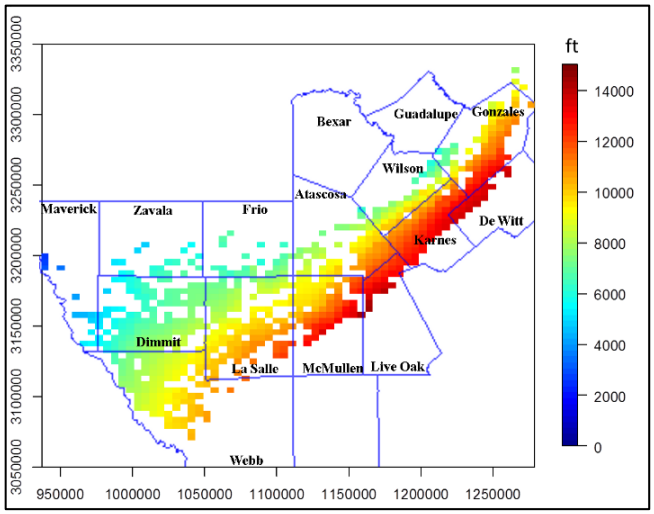

Fig. 13 Depth of Lower Eagle Ford Shale base predicted for Eagle Ford production wells locations by kriging.

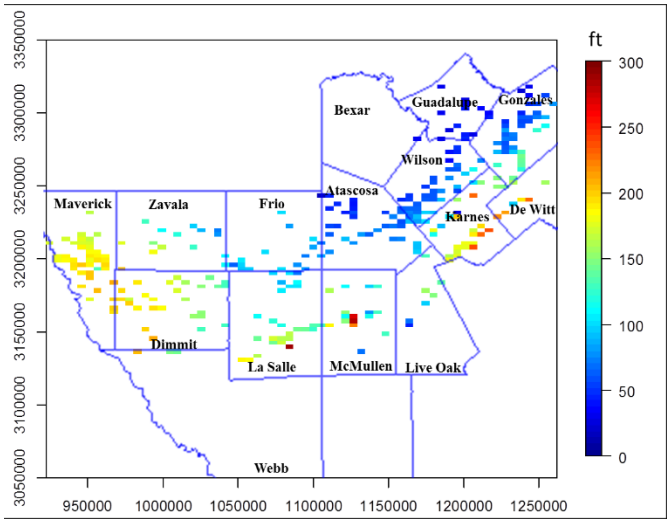

Fig. 14 Thickness of Lower Eagle Ford Shale by stratigraphic analyses on vertical wells.

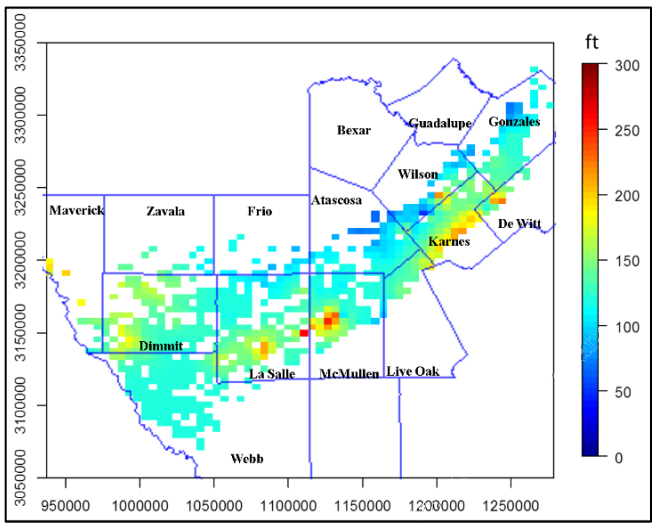

Fig. 15 Thickness of Lower Eagle Ford Shale predicted for Eagle Ford production well locations by kriging.

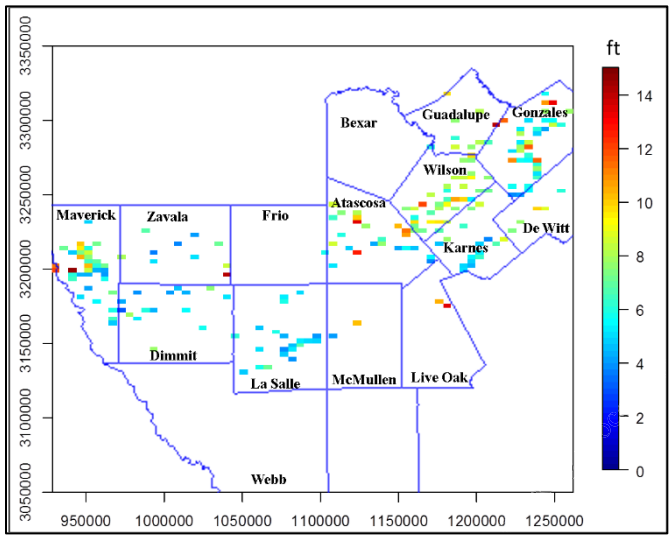

Fig. 16 Average bed thickness of Lower Eagle Ford Shale calculated at vertical wells.

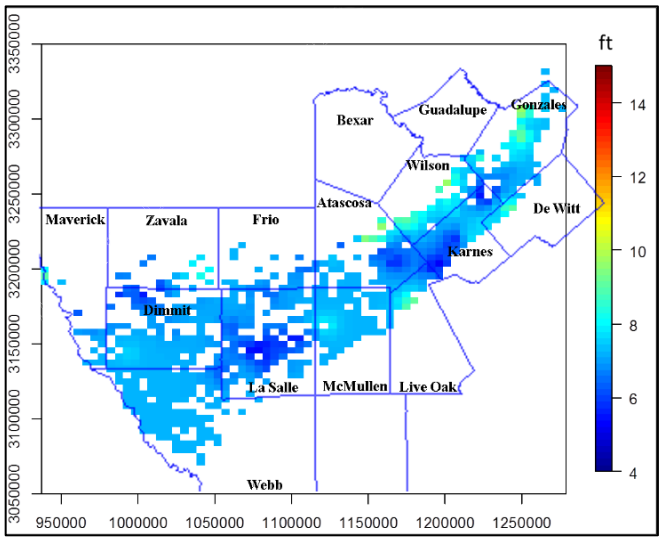

Fig. 17 Average bed thickness of Lower Eagle Ford Shale predicted for Eagle Ford well locations by kriging.

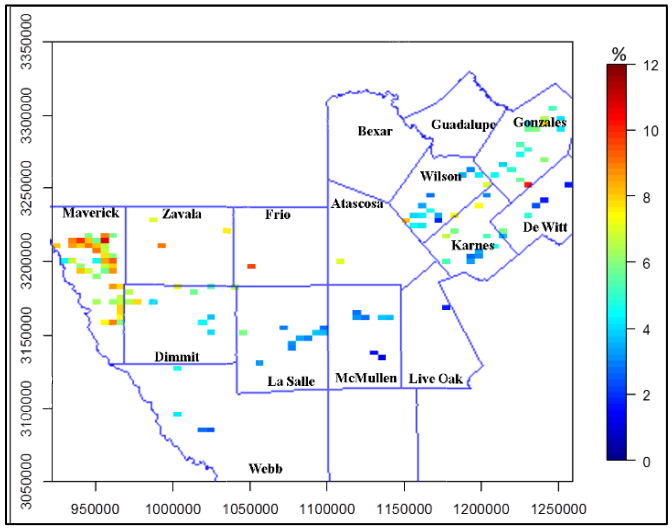

Fig. 18 TOC calculated at vertical wells by petrophysical analyses

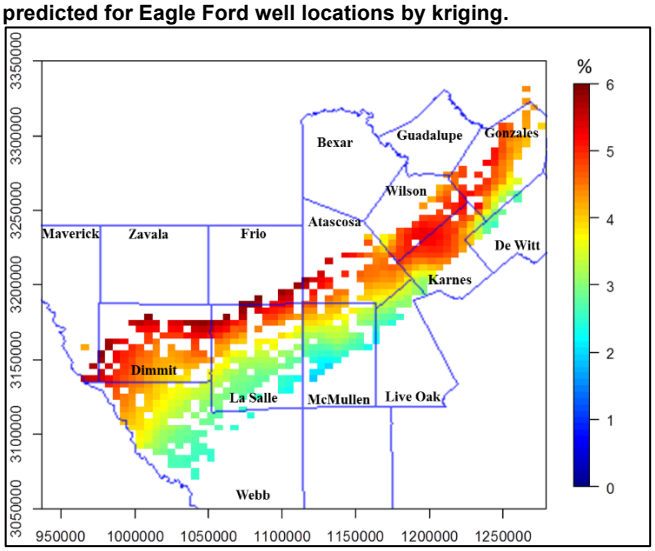

Fig. 19 TOC predicted for Eagle Ford well locations by kriging.

Poisson Distribution Prediction

The Q-Q plot of the number of limestone beds indicates the discrete and discontinuous character of limestone beds and, therefore, a Poisson distribution (**Fig. 20**). The MCMC chain trace plots illustrated the convergence of multiple chains within our proposed number of iterations. The convergence of three chains and the narrow density distribution demonstrated that the sampling results provided sufficiently reliable posterior results of β, σ^2, and ϕ (**Fig. 21**). With these posterior results we then predicted the number of limestone beds for Eagle Ford production wells from the vertical well data (**Figs. 22 and 23**).

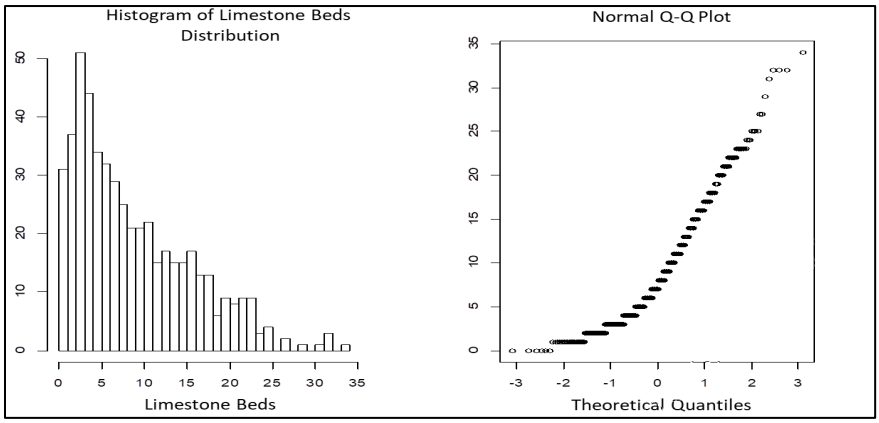

Fig. 20 Histogram and Q-Q plot of number of limestone beds.

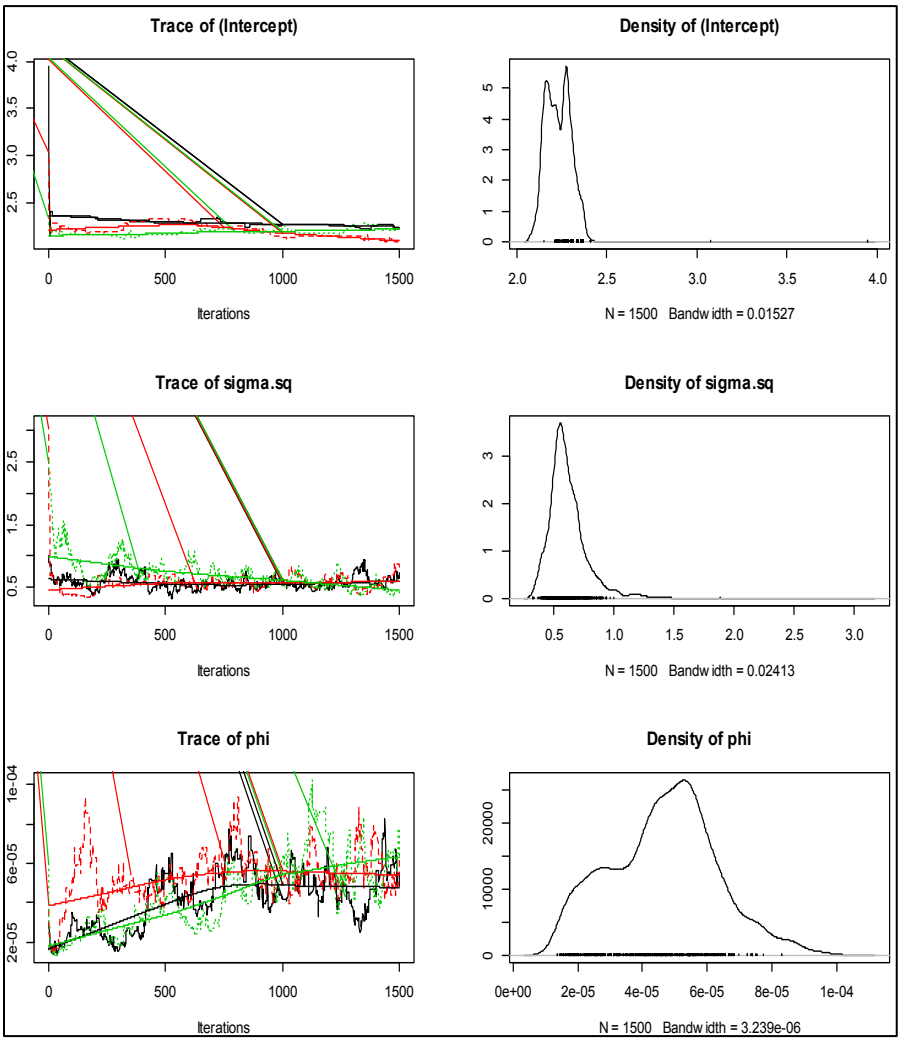

Fig. 21 MCMC sampling of intercept (β), variance (σ2), and spatial range (ϕ) for the number of limestone beds.

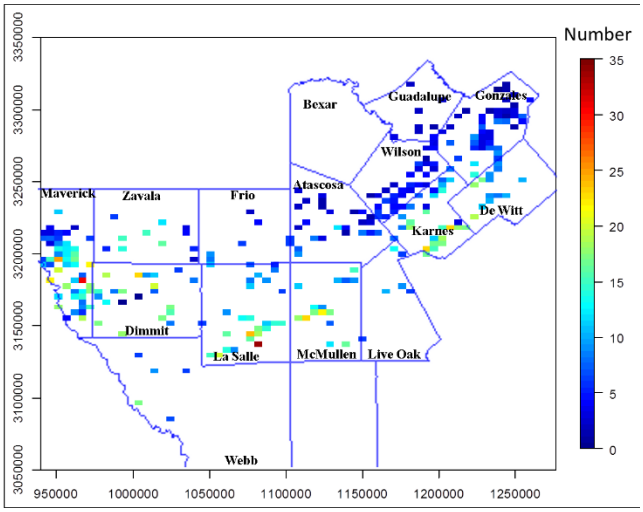

Fig. 22 Number of limestone beds at vertical wells.

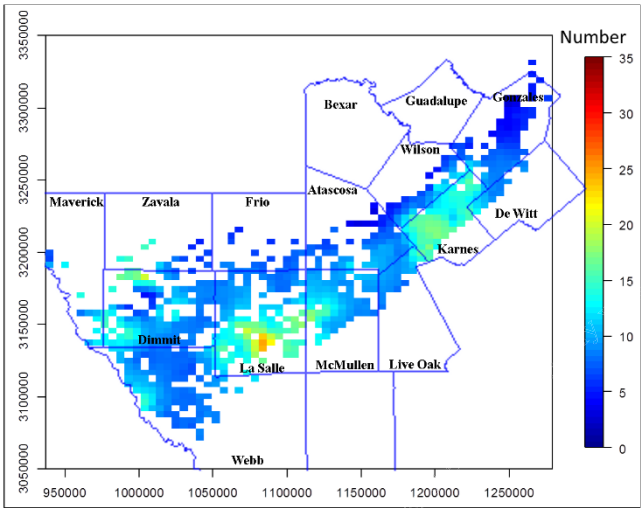

Fig. 23 Bayesian prediction of number of limestone beds at Eagle Ford production well locations.

Fitting Regression Models

The results from the previous steps gave geological data for the Eagle Ford horizontal production well locations (**Fig. 24**). Next, we fit the results with a regression model and quantified the linear relations between production and geologic parameters. After testing several models, we used a linear regression model to evaluate the relations between geological parameters and production. The model uses latitude and longitude positions reported in public databases containing the geological and production data values. The linear regression satisfies

$$Y = X\beta + \epsilon, \tag{6}$$

where β is a vector containing the regression model coefficients, X denotes a regressor matrix, ϵ is error term, and Y is the matrix containing known outputs, in this case six month cumulative production. If the linear regression model is a second order polynomial, the regressor matrix can be written as

$$X = (1, geo, geo^2), \tag{6}$$

where geo denotes the geological data parameters (Gelfand et al. 2010). The β vector values are quantified using the Levenberg-Marquardt (LM) algorithm available in the R software.

The following steps were necessary to achieve a more accurate model for production data:

Step 1. Polynomial Model: Production initially increases with depth, but after a certain level, production decreases with increasing depth as the formation enters the over-mature gas window. A polynomial model is required to capture these typical production data behaviors.

Step 2. Normalized Production Polynomial Model: As for previous parameters, the production data is normalized using the Box-Cox method, resulting in λ = 0.4. The Q-Q plots indicate that the production data are skewed before transformation and are symmetrical afterward (Fig. 24).

Step 3. Scaled Geological Data Normalized Production Polynomial Model: Because the values of the five geological parameters that had primary control on the regional production variations have very different ranges, it is not straightforward to know which parameters exert the greatest influence on cumulative production simply by comparing the magnitudes of the regression coefficients. To address this point, the geological parameters are normalized by dividing by the largest value thereby scaling all of them between 0 and 1.

With this regression model, we predicted the cumulative 6 month BOE (**Fig. 25**) and calculated the residuals between the predicted production and the observed production. Justification for these steps is easily seen by comparing the residuals resulting without and with them, which were 2 bbl and 600 bbl, respectively.

The regression also produces a p-value for each parameter. The p-value is the probability of obtaining a test statistic at least as extreme as the one that was actually observed, and have value 1 when t the null hypothesis is true, that is when there is no correlation. The p-value can be used to reject the null hypothesis when it is less than a certain significance level, often 0.05 (Gelfand et al. 2010). Therefore, small p-value implies a strong correlation.

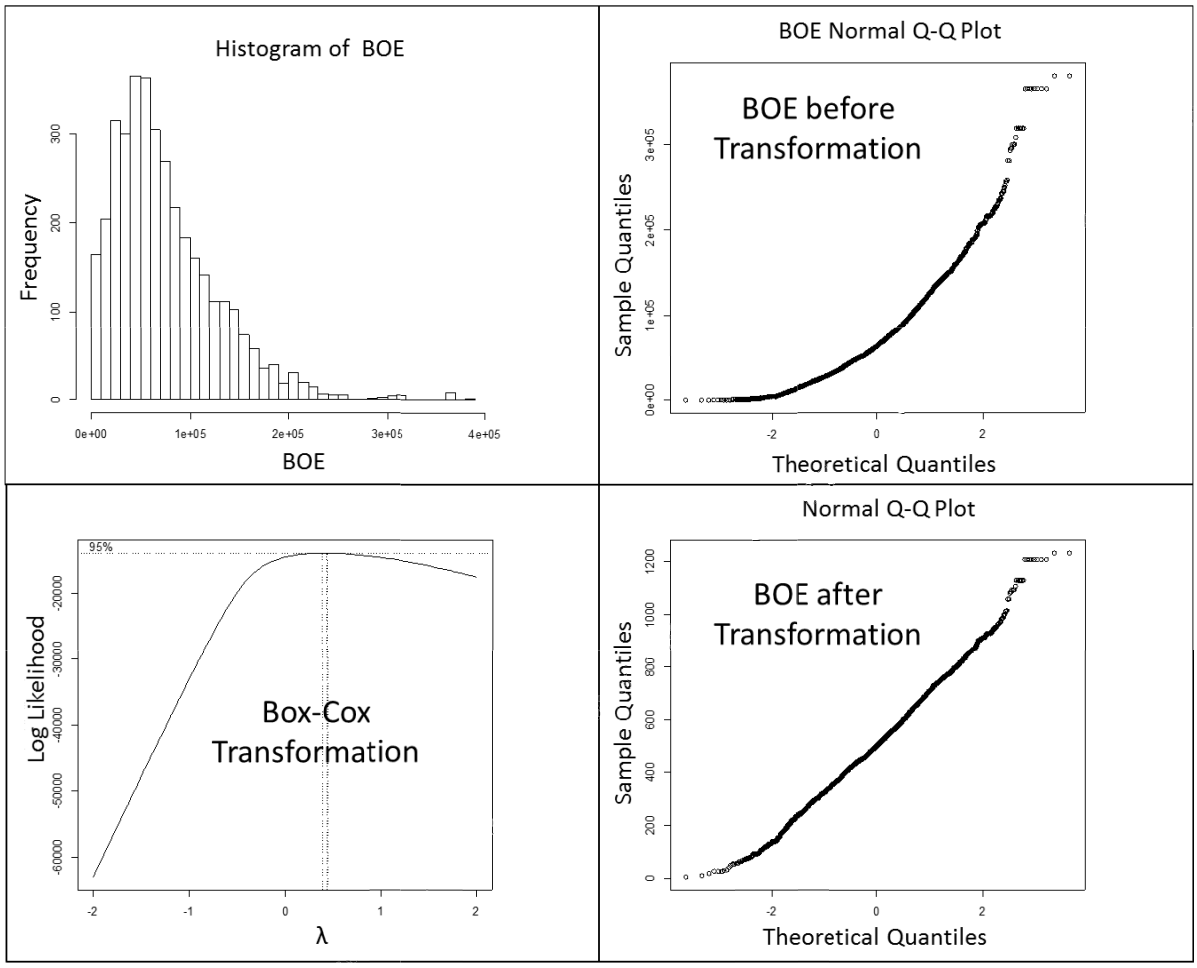

Fig. 24 Transformation of production data for Gaussian distribution without skewness.

Regression Result Interpretation

The regression fit for the data provides p-values and coefficients listed in **Table 1**. Both provide meaningful analysis.

P-value Analyses

In this project, p-values are important to understanding the significance level of the data and measuring the weight of the geological data. The longitude and latitude coordinates have high p-values, which indicates there is no relationship between production and these parameters. Depth, thickness, limestone bed number, and average bed thickness have low p-values, which suggests statistical significance of the relationship between production and these parameters. Table 1 shows significance codes for each parameter with *** indicating highest correlation significance.

The p-value analysis indicates that the most significant parameters to production are TOC and depth. The number of limestone beds also plays an important role, but it is less significant than other properties. Thickness plays a moderate role in production.

Coefficient Analysis

The coefficients of depth, thickness, average bed thickness, TOC, and number of limestone beds from the regression model are compared in **Table 2**. The coefficients could be used to analyze the relative

importance on production of each geological parameter since the geological parameters have been converted and range from 0 to 1.

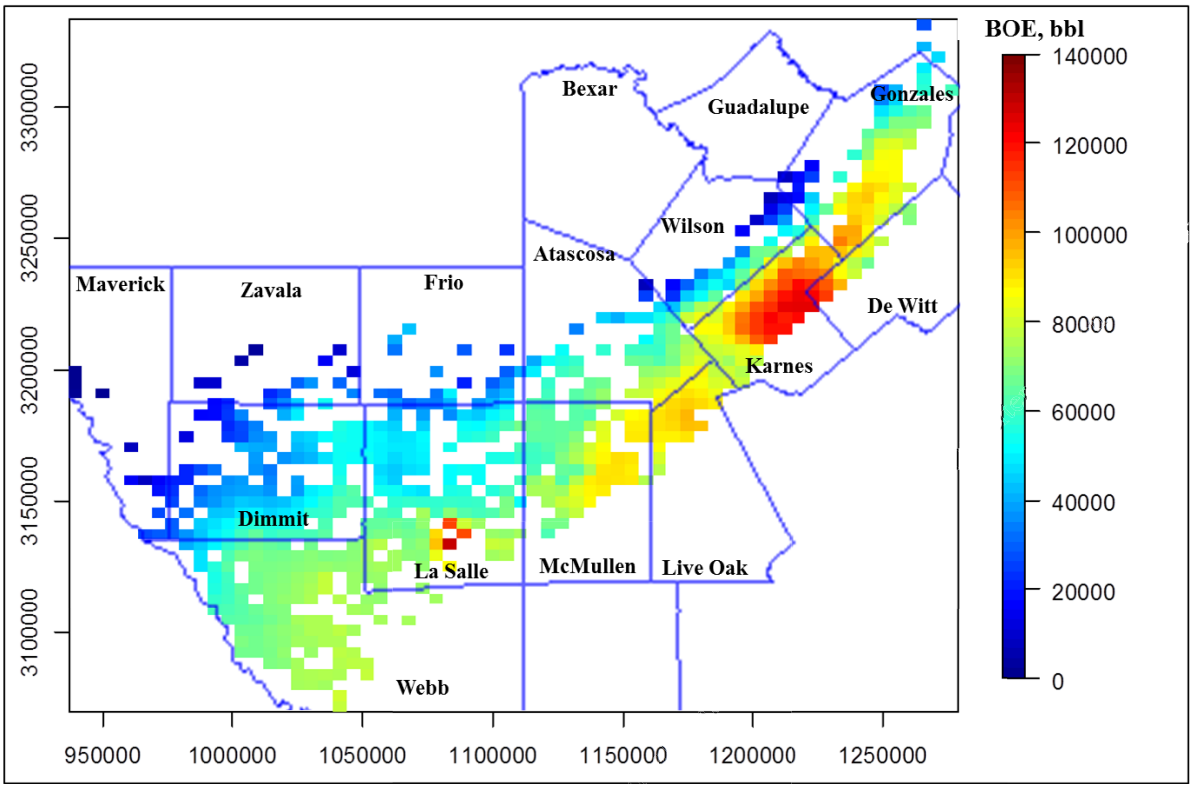

Fig. 25 First 6 months' production prediction (BOE).

TABLE 1 P-VALUES AND SIGNIFICANT CODES OF GEOLOGICAL PARAMETERS

	p-Value	Significance Code
Depth	< 2e-16	***
Depth^2	4.10E-09	***
Thickness	6.63E-07	***
Thickness^2	2.08E-06	***
TOC	< 2e-16	***
TOC^2	5.65E-15	***
Number of Limestone Beds	3.62E-11	***
Number of Limestone Beds^2	5.67E-12	***
Average Bed Thickness	1.21E-04	**
Average Bed Thickness^2	5.57E-04	**
X Coordinate	0.168047	
Y Coordinate	0.105604	

TABLE 2 THE COEFFICIENTS OF GEOLOGICAL PARAMETERS FROM REGRESSION	
Depth	2.37E+03
Depth^2	-1.06E+03
Thickness	1.19E+03
Thickness^2	-1.03E+03
TOC	1.72E+03
TOC^2	-1.30E+03
Number of Limestone Beds	-9.01E+02
Number of Limestone Beds^2	9.84E+02
Average Bed Thickness	2.60E+03
Average Bed Thickness^2	-1.66E+03

The maximum coefficients are from depth and average bed thickness of the Lower Eagle Ford, which suggests that these two parameters play the most significant roles in production. The following discussion holds the other parameters constant, and shows plots of each geological parameter against production using the coefficient. This allowed further investigation into the relationships between production and these parameters.

Depth vs. BOE Production

Plotting the first 6 months' production against depth (elevation, subsea level) using the coefficient achieved from regression shows that production increases with structural depth throughout the entire study area (**Fig. 26**).

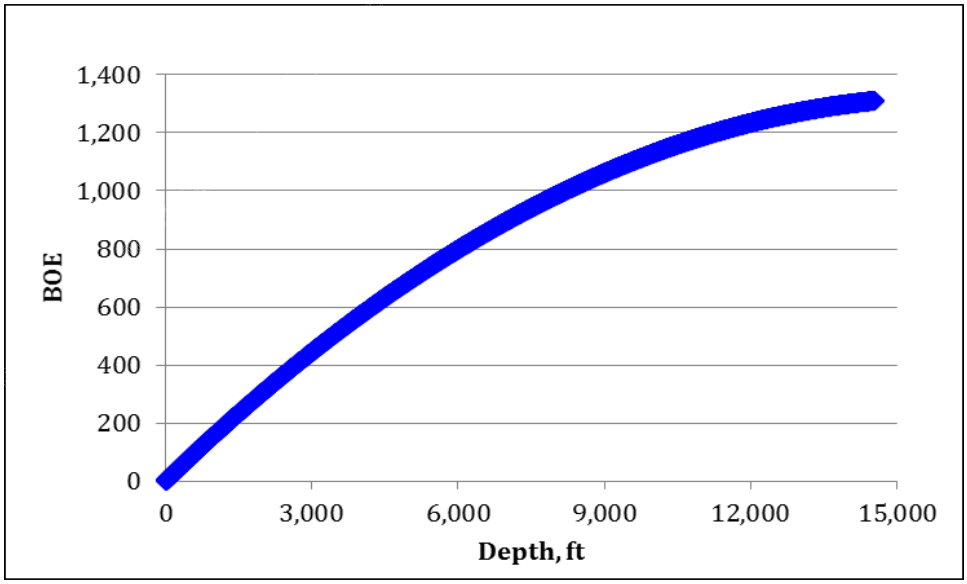

Fig. 26 Depth vs. production correlation of regression.

Thickness vs. BOE

Production increases with thickness until the thickness reaches 180 ft. Where the Lower Eagle Ford is thicker than 180 ft, production declines (**Fig. 27**). This is reasonable and consistent with observations,

because thickness exceeds 180 ft mainly in the Maverick basin depocenter (Fig. 2), where production is relatively low, compared to the rest of the study area (Fig. 8).

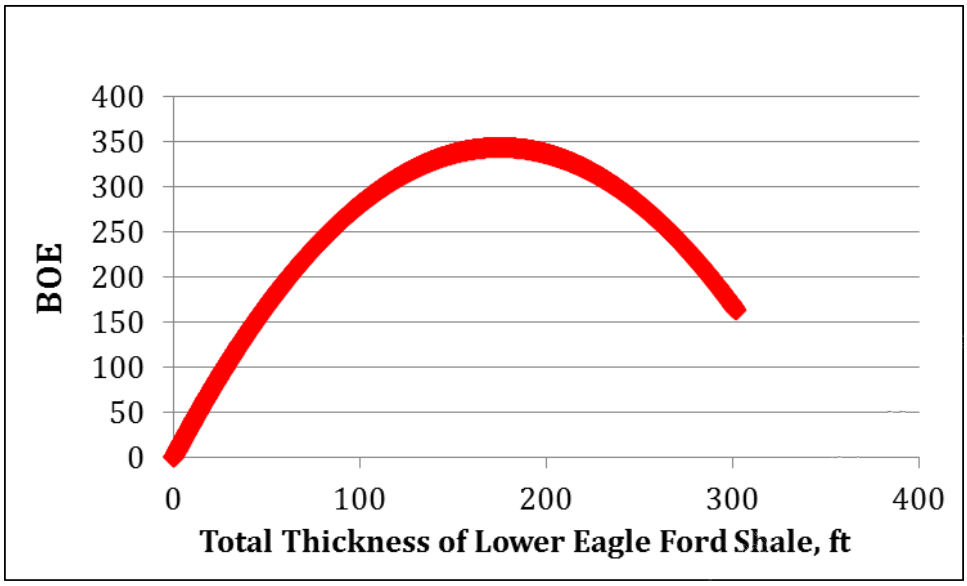

Fig. 27 Total thickness of Lower Eagle Ford Shale vs. production correlation of regression.

TOC vs. BOE Production

Production from initial 6 months increases with TOC until TOC exceeds approximately 7%. Where TOC exceeds 7%, production decreases with TOC (**Fig. 28**). Several factors may result in such a relationship. TOC greater than 7% may suggest low thermal maturity or highly ductile rock, both of which have a negative role in overall production.

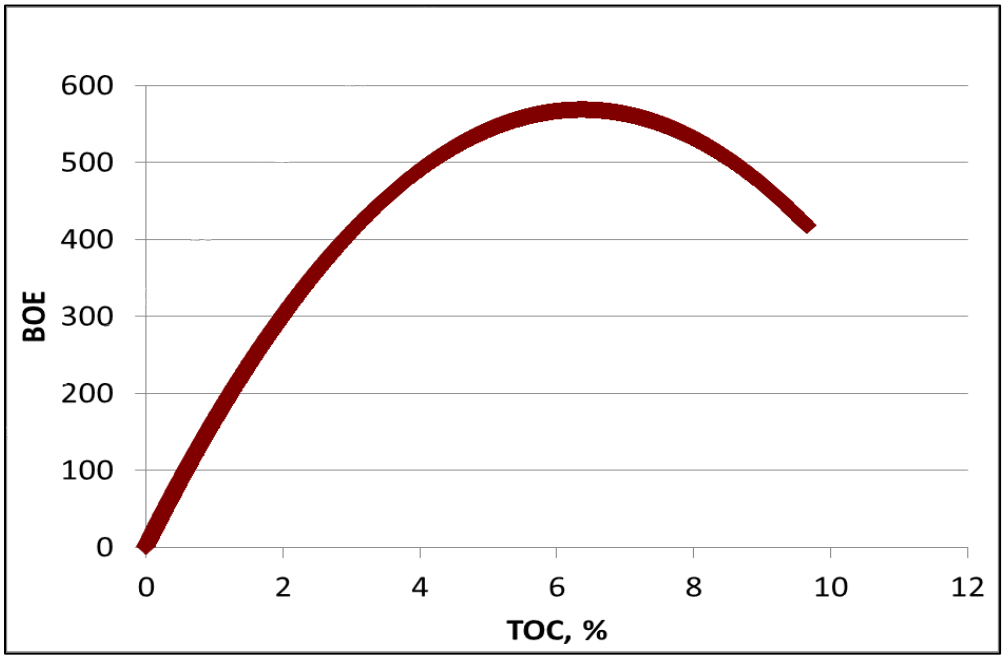

Fig. 28 Average TOC of Lower Eagle Ford Shale vs. production correlation of regression.

Number of Limestone Beds vs. BOE Production

A plot of production against the number of limestone beds showed a decreasing and an increasing pattern (**Fig. 29**). In the study area, oil production increases with the number of limestone beds. In the northern study area where the total number of limestone beds is less than 12, the correlation between production and number of limestone beds is quite complex, and overall, it negatively impacts the production, regionally. In the southern study area, where the number of limestone beds exceeds 12, production is higher (Fig. 28).

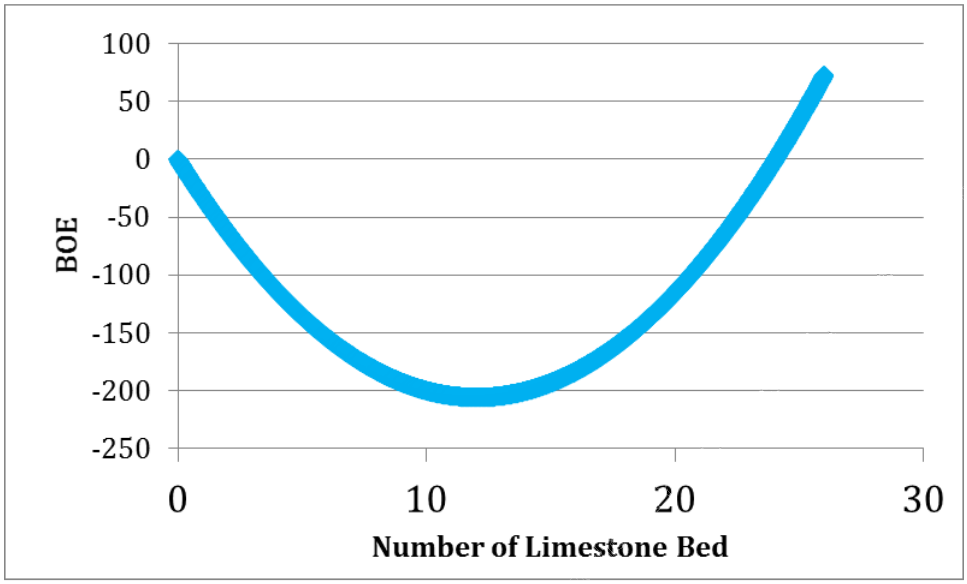

Fig. 29 Number of limestone beds in Lower Eagle Ford Shale vs. production correlation of regression.

Average Bed Thickness vs. BOE Production

Production increases with average bed thickness, up to bed thickness of approximately 7 ft (**Fig. 30**).

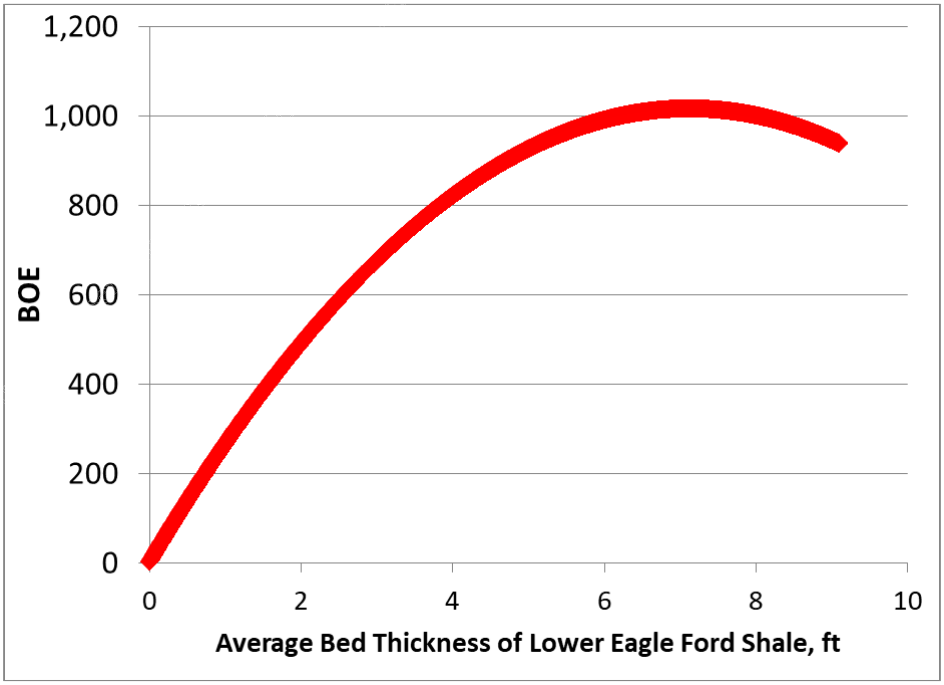

Fig. 30 Average bed thickness of Lower Eagle Ford Shale vs. production correlation of regression.

Kriging Limitations

Kriging may be used with nearby data to predict geological parameters at locations where no measured values are available. It is especially useful when limited well control is present. However, kriging based on a stationary covariance function has limitations when applied to a large area. Kriging interpolates values for unknown locations without considering the possible local heterogeneity in geological parameters. Without sufficient sample density, local geological variability will not be accurately detected, and thus, considerable geological details may be lost during kriging.

Discussion

This paper provides quantitative analyses of which geological parameters exert dominant controls on regional hydrocarbon production trends in the Eagle Ford Shale play. The results are geologically intuitive and consistent.

Depth is the dominant control on the first 6 months production of the Eagle Ford Shale. Productivity of Eagle Ford shale increases with depth, which in turn, is related to increasing formation temperature, pressure, and thermal maturity. With increasing thermal maturity and temperature, more organic material is converted to hydrocarbon, hydrocarbon viscosity decreases, and more water was expelled from the source rock, leading to higher hydrocarbon saturation and lower water saturation (Baskin 1997; Curtis 2002; Zhao et al. 2007; Wang and Gale, 2009; Passey et al. 2010;). Increasing depth and temperature contributed to higher level of diagenesis and TOC conversion, which enhanced formation brittleness (Wang and Gale 2009). In the gas window, although the absorbed gas content and free gas content are also related to TOC and porosity, at greater depth in the Eagle Ford, the higher reservoir pressure contributes to production by increasing the absorption capacity and free gas compressibility.

TOC is a critical productivity parameter for the Eagle Ford Shale. Previous workers have demonstrated strong correlation between TOC and the total porosity as well as gas content, using core data from more than 10 shale-gas formations worldwide (Passey et al.2010; Dicman and Vernik, 2013; Wang and Carr, 2013; Wang et al.2013). However, our results show the correlation between TOC and productivity is not monotonic, which suggests in the Eagle Ford Shale there is an upper limit beyond which more organic material would not contribute positively with productivity. When the TOC exceeds certain value, 7% in Eagle Ford Shale, the ductile nature of organic material causes the reservoir unfavorably responding to hydraulic fracture propagation, and thus, excessively high organic richness would significantly negatively impact stimulation efficiency and well productivity (Baruch et al.2012; Clarke et al.2016).

Thickness exercises control of shale oil and gas production by controlling the volume of hydrocarbons in place. The maximum number of limestone beds coincides with the most productive Eagle Ford Shale regions. Previous researchers have thoroughly investigated the correlation between the stimulation efficiency and mineral composition, especially the composition of the brittle minerals. A positive correction between permeability and calcite composition (limestone) was found in Eagle Ford Shale (Kosanke and Warren, 2016). Sufficient amount of calcite is crucial to Eagle Ford shale production (Jarvie et al.2007; Rickman et al.2008; Sondergeld et al.2010; Baruch et al.2012; Wang and Carr, 2013). However, our results show an initial trend of decreasing productivity of first 6 months production and the number of limestone beds. High concentration of calcite leads to more efficient fracture simulation; however, it also reduces the volume of hydrocarbon-saturated pay zone while holding the total volume constant (Baruch et al.2012; Clarke et al.2016). These results suggest that optimum productivity may be expected where there is a balance of sufficient organic-rich intervals with higher porosity (hydrocarbons storage capacity) and brittle limestone beds that facilitate hydraulic fracturing.

Finally, the parameters selected in our study are restricted to regional geological parameters. We did not account for the effects of local faults, folds, or stress variations. We that realize the completion and stimulation strategies change with time and operator, even within the same shale play. However, the first

production date of the wells used in this study is concentrated in 2011 and 2012. We compared the cumulative first 6 months of production among wells with different initial production dates, and even though there are a few outliers in late 2012 showing high production, the limited number of such samples should have little statistical impact on our regional analysis. Individual well failure or success would not affect the overall regional trend. However, because the completion and stimulation designs vary among operators within the same time window, it would be worthwhile to include these parameters in the next stage of analysis.

Conclusions

Statistical methods were used to infer geological properties at horizontal well locations on the basis of those properties of nearby vertical wells; then, statistical analyses successfully demonstrated regional geologic controls on horizontal well productivity. The 6-month cumulative production (BOE) of the Eagle Ford Shale increases consistently with depth, lower Eagle Ford thickness (up to 180-ft thickness), and TOC (up to 7%). The corresponding significance code levels indicates that the most significant parameters to production are TOC and depth (which relates to pressure). The number of limestone (brittle) beds also plays an important role, but it is less significant than other properties. In the northwestern region, where the total number of limestone beds is fewer than 12, cumulative production is low. In the southeastern region, where the number of limestone beds exceeds 12, production increases with the number of limestone beds. P values analyses suggest high certainty of the relationship between the production and five reservoir parameters tested in the regression model.

The sustained low equity price since 2015 has created a challenging economic environment for shale development. However, organic-rich shale plays will continue to be a vital source of energy for the U.S. and to the rest of the world in the future. The approach developed in this study may assist operators in making critical Eagle Ford Shale development decisions, and this approach may be transferable to other shale plays.

Nomenclature

λ = power transformation parameter
$Y(x)$ = the observed data at spatial location x
μ = the mean value of the data set
S = spatial random effect modeled by a Gaussian process
e = error term
K = covariance function
α = sill
β = the spatial range
ν = smoothness parameter
κ_ν = the Bessel function of second kind
λ = the non-Gaussian data
S_i = specific site
η = a Gaussian latent process
β = random variable
σ^2 = variance
ϕ = latent spatial range
β = vector containing the regression model coefficients
X = denotes a parameter matrix
ϵ = error term
Y = the matrix containing known outputs

References

Banerjee, S., Carlin, B.P., and Gelfand, A.E. 2004. Hierarchical Modeling and Analysis For Spatial Data, Chapman and Hall/CRC press, Boca raton, Fla.

Banerjee, S., Gelfand, A.E., Finley, A.O. et al. 2008. Gaussian Predictive Process Models for Large Spatial Datasets. Journal of the Royal Statistical Society Series B, 70:825–848.

Baskin, D. K. 1997. Atomic H/C ratio of kerogen as an estimate of thermal maturity and organic matter conversion: American Association of Petroleum Geologists Bulletin, v. 81, no. 9, p. 1437–1450, doi:10.1306/3B05BB14-172A-11D7-8645000102C1865D

Baruch, E. T., Slatt, R. M. and Marfurt, K. J. 2012. Seismic Stratigraphic Analysis of the Barnett Shale and Ellenberger Unconformity Southwest of the Core Area of the Newark East Field, Fort Worth Basin, Texas, in J. A. Breyer, ed., Shale Reservoirs—Giant Resources for the 21st Century: AAPG Memoir 97: p. 403–418. doi:10.1306/13321483M97441.

Bohm, G. and Zech, G. 2010. Introduction to Statistics and Data Analysis for Physicists. Verlag Deutsches Elektronen-Synchrotron.

Box, G.E. and Cox, D.R. 1964. An analysis of transformation. Journal of the Royal Statistical Society 26:211-252.

Bowker, K. A. 2003. Recent Development of the Barnett Shale Play, Forth Worth Basin: West Texas Geol Soc Bull, v(2000), p. 6.

Bowker, K. A. 2007. Barnett Shale gas production, Fort Worth Basin: Issues and discussion: AAPG Bulletin, 91(4): 523–533, doi:10.1306/06190606018.

Cipolla, C., Weng, X., Onda, H. et al. 2011. New Algorithms and Integrated Workflow for Tight Gas and Shale Completions. Presented at SPE Annual Technical Conference and Exhibition, Denver, Colorado, 30 October-2 November. SPE -146872-MS. http://dx.doi.org/10.2118/146872-MS.

Clarke, P. R., D. H. Portis, G. J. Barzola, H. Bello, and N. K. Basu, 2016, Chapter 5: Assessing Well Performance in a Prolific Liquids-rich Shale Play—An Eagle Ford Case Study, in J. A. Breyer, ed., The Eagle Ford Shale: A renaissance in U.S. oil production: AAPG Memoir 110: p. 213–240. doi:10.1306/13541963M1103662.

Curtis, J. B. 2002. Fractured Shale-gas Systems: AAPG Bulletin, 86(11): 1921–1938. doi:10.1306/61EEDDBE-173E-11D7-8645000102C1865D

Davis, D., and Reynold, S. J. 1996. Structural geology of rocks and regions, 2nd ed.: Wiley, New York, 776 p.

Dicman, A. and Vernik, L. 2013. A New Petrophysical Model for Organic Shales: Petrophysics, 54(3), 1–15.

EIA. 2011. Review of Emerging Resources: U.S. Shale Gas and Shale Oil Plays. Report Retrieved in March 2013. http://www.eia.gov/analysis/studies/usshalegas/full report errata (accessed July 2011)

EIA. 2012. Review of Emerging Resources: U.S. Shale Gas and Shale Oil Plays Report Retrieved in March 2013. http://www.eia.gov/naturalgas/review/production.cfm

EIA. 2014. U.S. Crude Oil and Natural Gas Proved Reserves. Report Retrieved in January 2015. https://www.eia.gov/naturalgas/crudeoilreserves/archive/2013/index.php

EIA. 2016. U.S. Crude Oil and Natural Gas Proved Reserves, Year-end 2015. Report Retrieved in January 2017. https://www.eia.gov/naturalgas/crudeoilreserves/

Finley, A.O., Banerjee, S., and Roberts, R.E. 2008. A Bayesian Approach to Quantifying Uncertainty in Multi-Source Forest Area Estimates. Environmental and Ecological Statistics, 15:241–258.

Finley, A.O., Banerjee, S., Gelfand, A.E. 2015. spBayes for Large Univariate and Multivariate Point-Referenced Spatio-temporal Data Models. Journal of Statistical Software, 63:1-28

Gelfand, A., Diggle. P., and Guttorp, P. et al. 2010. Handbook of Spatial Statistics. CRC Press.

Handin, J. and Hager, R. V. 1957. Experimental Deformation of Sedimentary Rocks Under Confining Pressure: Tests at Room Temperature on Dry Samples: American Association of Petroleum Geologists Bulletin, 41(1):1-50.

Handin, J., Hager, R. V., and Friedman, M. et al. 1963. Experimental deformation of sedimentary rocks under confining pressure: Pore pressure tests: American Association of Petroleum Geologists Bulletin, 47(5): 717-755.

Hentz, T. H. and Ruppel, S. C. 2010. Regional lithostratigraphy of the Eagle Ford Shale: Maverick Basin to East Texas Basin. Gulf Coast Association of Geological Societies Transactions 60: 325-338.

Hill, D. G., and Nelson, C. R. 2000, Gas Productive Fractured Shales—An Overview and Update: GasTIPS, 7(2): 11– 16.

Huang, S., Yang, Q., and Matuszyk, P. J. et al. 2013. High-Resolution Interpretation of Sonic Logging Measurements Using Stochastic Inversion with Spatial Slowness Sensitivity Functions. Presented at 2013 SEG Annual Meeting, 22-27 September, Houston, Texas. https://doi.org/10.1190/segam2013-0051.1

Huang, S. and Torres-Verdín, C. 2015. Sonic Spatial Sensitivity Functions and Inversion-Based Layer-by-Layer Interpretation of Borehole Sonic Logs. Presented SPWLA 56th Annual Logging Symposium, 18-22 July, Long Beach, California, USA. SPWLA-2015-S.

Jarvie, D. M., Hill, R. J., and Ruble, T. E. et al. 2007, Unconventional Shale-gas Systems: The Mississippian Barnett Shale of North-Central Texas as One Model for Thermogenic Shale-gas Assessment: AAPG Bulletin, 91(4): 475–499. doi:10.1306/12190606068.

Krige, D. and Kleingeld, W. 2005. The genesis of geostatistics in gold and diamond industries, in the proceedings of P. Bickel, P. Diggle, S. Fienberg, U. Gather. 2005. Lecture Notes in Statistics. Springer.

Loucks, R. G. and Reed, R. M. 2014, Scanning-electron-microscope Petrographic Evidence for Distinguishing Organic-matter Pores Associated with Depositional Organic Matter Versus Migrated Organic Matter In Mudrocks: GCAGS Journal, v. 3, p. 51–60

Montgomery, S. L., Jarvie, D. M., and Bowker, K. A. et al. Mississippian Barnett Shale, Fort Worth basin, north-central Texas: Gas-shale play with multi-trillion cubic foot potential: AAPG Bulletin, 89(2):155–175. doi:10.1306/09170404042.

Mullen, J. 2010. Petrophysical Characterization of the Eagle Ford Shale in south Texas. Presented at Canadian Unconventional Resources & Petroleum Conference, Calgary, Alberta, Canada, 19-21 October. SPE-138145 –MS. http://dx.doi.org/10.2118/138145-MS.

Mullen, J., Lowry, J.C., and Nwabuoku, K.C. 2010. Lesson Learned Developing the Eagle Ford Shale. Paper presented Tight Gas Completions Conference in San Antonio, Texas, 18-20 March. SPE-138446 -MS. http://dx.doi.org/10.2118/138446-MS

Passey, Q.R., Creaney, S., and Kulla, J.B. et al. 1990. A Practical Model for Organic Richness from Porosity and Resistivity Logs. AAPG Bulletin 74 (12): 1777-1794.

Passey, Q.R., Bohacs, K.M., and Esch, W.L. et al. 2010. From Oil-Prone Source Rock to Gas-producing Shale Reservoir-Geologic and Petrophysical Characterization of Unconventional Shale Gas Reservoirs. Presented at International Oil and Gas Conference and Exhibition in Beijing, China, 8-10 June. SPE- 131350-MS.

http://dx.doi.org/10.2118/131350-MS.
Peters, K. E. and Cassa, M. R. 1994, Applied Source Rock Geochemistry, *in* Magoon, L. B, and W. G. Dow, eds., 1994, The petroleum system-from source to trap: AAPG Memoir 60.: p. 93–120
Pollastro, R. M., Jarvie, D. M., Hill, R. J. et al. 2007, Geologic Framework of the Mississippian Barnett Shale, Barnett-paleozoic Total Petroleum System, Bend Arch-Fort Worth Basin, Texas: AAPG Bulletin, 91(4): 405–436, doi:10.1306/10300606008
Quirein, J., Witkowsky, J., and Truax, J. A. et al. 2010, Integrating Core Data and Wireline Geochemical Data for Formation Evaluation and Characterization of Shale-Gas Reservoirs: Presented at SPE Annual Technical Conference and Exhibition, Florence, Italy, 19–22 September 2010. SPE-134559-MS.
http://dx.doi.org/10.2118/134559-MS.
Quirein, J., Praznik, G., and Galford, J. et al. 2013. A Workflow to Evaluate Mineralogy, Porosity, TOC, and Hydrocarbon Volume in the Eagle Ford Shale. Presented at SPE Unconventional Resources Conference and Exhibition-Asia Pacific, Brisbane, Australia, 11-13 November. SPE- 167012-MS.
http://dx.doi.org/10.2118/167012-MS.
R [Computer Software]. 2013. Retrieved from https://www.r-project.org/.
Ramirez, T., Klein, J., and Bonnie, R. et al. 2011. Comparative Study of Formation Evaluation Methods for Unconventional Shale Gas Reservoirs: Application to the Haynesville Shale (Texas). Presented at North American Unconventional Gas Conference and Exhibition, Woodlands, Texas, USA, 14-16 June. SPE-144062-MS.
http://dx.doi.org/10.2118/144062-MS.
Ribeiro, P. J. Jr. and Diggle P. J. 2016. Package geoR. Retrieved from https://cran.r-project.org/web/packages/geoR/geoR.pdf in June 2016.
Rickman, R., Mullen, M, and Petre, E. et al. 2008. A Practical Use of Shale Petrophysics for Stimulation Design Optimization: All Shale Plays Are Not Clones of the Barnett Shale. Presented SPE Annual Technical Conference and Exhibition, Denver, Colorado, 21-24 September. SPE-115258-MS.
http://dx.doi.org/10.2118/115258-MS.
Roberts, C. and Casella, G. 2004. Monte Carlo Statistical Methods. Springer-Verlag New York. ISBN: 978-0-387-21239-5.
Roberts, G.S. and Rosenthal, J.S. 2006. Examples of Adaptive MCMC. http://probability.ca/ieff/ftpdir/adaptex.pdf.
Rivoirard, J. 2005. Concepts and methods of Geostatistics, in the proceedings of P. Bickel, P. Diggle, S. Fienberg, U. Gather. 2005. Lecture Notes in Statistics. Springer.
Scott D, Lane DM .2008 Box-Cox transformations online statistics education: a multimedia course of study. http://onlinestatbookcom/.
Skbkekas.2009 Normal quantile plot of a set of 100 independent standard exponential values
http://enwikipediaorg/wiki/File:Normal_exponential_qqsvg.
Sondergeld, C. H., Newsham, K. E., and Comisky, J. T. 2010, Petrophysical Considerations in Evaluating and Producing Shale Gas Resources. Presented at SPE Unconventional Gas Conference, Pittsburgh, Pennsylvania, USA, 23–25 February. SPE -131768-MS.
http://dx.doi.org/10.2118/131768-MS.
Spears, R.W. and Jackson S. L. 2009. Development of a Predictive Tool for Estimating Well Performance in Horizontal Shale Gas Wells in the Barnett Shale, North Texas, USA. Petrophysics 50 (1): 19-31.
Sun, T., Merletti, G. Patel, H. et al. 2015, Advanced Petrophysical, Geological, Geophysical and Geomechanical Reservoir Characterization - Key to the Successful Implementation of a Geo-Engineered Completion Optimization Program in the Eagle Ford Shale. Presented at the Unconventional Resources Technology Conference, San Antonio, Texas, USA, 20–22 July. Paper-178524-MS.
http://dx.doi.org/10.15530/urtec-2015-2152246.
TRC (Texas Railroad Commission). 2014. Texas Eagle Ford Shale drilling permit issued each year.
https://wwwrrcstatetxus/eagleford/EagleFordDrillingPermitsIssuedpdf (accessed February 2014).
Tian, Y., Ayers, W. B., and McCain, W. D. Jr. 2012. Regional Analysis of Stratigraphy, Reservoir Characteristics, and Fluid Phases in the Eagle Ford Shale. Presented at Gulf Coast Association of Geological Societies and the Gulf Coast Section of SEPM, Austin, Texas, 21-24 October.
Tian, Y., Ayers, W.B., and McCain, W.D. Jr. 2013. The Eagle Ford Shale Play, South Texas: Regional Variations in Fluid Types, Hydrocarbon Production and Reservoir Properties. Presented at the International Petroleum Technology Conference, Beijing, China, 26–28 March. IPTC-16808-MS.
http://dx.doi.org/10.2523/IPTC-16808-MS
Tian, Y., Ayers, W. B., and McCain, W. D. Jr. 2014. Regional Impacts of Lithologic Cyclicity and Reservoir and Fluid Properties on Eagle Ford Shale Well Performance. Presented for SPE Unconventional Resources Conference, Woodlands, TX, 1-4 April. SPE-169007-MS.
http://dx.doi.org/10.2118/169007-MS
Wan, J., Barnum, R., DiGloria, D.C. et al. 2013. Factors Controlling Recovery in Liquid Rich Unconventional Systems. Presented at the International Petroleum Technology Convergence, Beijing, China, 26-28 March. IPTC-17103-MS.
http://dx.doi.org/10.2523/IPTC-17103-MS.
Wang, F. and Gale, J. 2009. Screening criteria for shale-gas system. Gulf Coast Association of Geological Societies Transactions, 59:779-793.
Wang, G., and Carr, T. R. 2013. Organic-rich Marcellus Shale Lithofacies Modeling and Distribution Pattern Analysis in the Appalachian Basin: AAPG Bulletin, 97(12): 2173–2205.
doi:10.1306/05141312135
Wang, F. P., Hammes, U., and Li, Q. 2013. Overview of the Haynesville Shale Properties and Production, in U. Hammes and J. Gale, eds., Geology of the Haynesville Gas Shale in East Texas and West Louisiana, U.S.A.: AAPG Memoir 105: p. 155–177.
doi:10.1306/13441848M1053527.
Wilk, M. and Gnanadesikan, R. 1968. Probability Plotting Methods for the Analysis of Data. Biometrika 55:1-17.
doi: 10.1093/biomet/55.1.1.

Yu, W., Huang, S., and Wu, K. et al. 2014. Development of a Semi-Analytical Model for Simulation of Gas Production in Shale Gas Reservoirs. Paper presented at Unconventional Resources Technology Conference, 25-27 August, Denver, Colorado, USA. URTEC-1922945-MS
doi:10.15530/URTEC-2014-1922945

Zhao, H., Givens, N. B., and Curtis, B. 2007. Thermal maturity of the Barnett Shale determined from well-log analysis. AAPG Bulletin, 91(4): 535– 549.
doi:10.1306/10270606060.